NATIONAL ADVISORY COMMITTEE FOR AERONAUTICS

WARTIME REPORT

ORIGINALLY ISSUED
February 1943 as
Advance Restricted Report

THE EFFECTS OF ANGLE OF DEAD RISE AND ANGLE OF AFTERBODY KEEL ON THE RESISTANCE OF A MODEL OF A FLYING-BOAT HULL

By Joe W. Bell and John M. Willis, Jr.

Langley Memorial Aeronautical Laboratory
Langley Field, Va.

NACA

WASHINGTON

NATIONAL ADVISORY COMMITTEE FOR AERONAUTICS

ADVANCE RESTRICTED REPORT

L-305

THE EFFECTS OF ANGLE OF DEAD RISE AND ANGLE OF AFTERBODY KEEL ON THE RESISTANCE OF A MODEL OF A FLYING-BOAT HULL

By Joe W. Bell and John M. Willis, Jr.

SUMMARY

A series of models of flying-boat hulls was tested in NACA tank no. 1 to determine the effects of the angle of dead rise and the angle of afterbody keel on resistance and spray characteristics. Three angles of dead rise, $14\frac{3}{4}^{\circ}$, 19°, and $23\frac{1}{4}^{\circ}$, and three angles of afterbody keel, 4°, $6\frac{1}{4}^{\circ}$, and $8\frac{1}{2}^{\circ}$, were investigated. The tests included nine configurations incorporating all possible combinations of these values. The results of the tests are expressed in nondimensional coefficients.

The effect of angle of dead rise on resistance and best trim was negligible up to and including the hump. At higher speeds, the resistance was reduced by the lower dead rise and increased by the higher dead rise. These differences, however, were relatively small.

At small angles of afterbody keel, the resistance was low at low speeds and high at planing speeds. The positive trimming moments were reduced by reducing the angle of afterbody keel. High angles of afterbody keel gave a higher best trim at the hump and at planing speeds.

The effects of angle of afterbody keel were consistent at all angles of dead rise and the effects of dead rise were consistent at all angles of afterbody keel.

An appendix showing the method used for deriving models of the 126A and 126C series from the basic model 126B-2 is included. Working charts for the determination of resistance and trimming moment for the model 126B-2 are also given.

INTRODUCTION

The purpose of the tests was to determine the effects of angle of afterbody keel and angle of dead rise on resistance and spray characteristics and to determine whether the effects of varying either of these angles are influenced by the value of the other angle.

The effects of the angle of afterbody keel and the angle of dead rise have been investigated separately in a number of earlier tests. The results of NACA investigations of the resistance effects of angle of afterbody keel and angle of dead rise have been reported in references 1 and 2, respectively. The experimental towing tank of Stevens Institute of Technology has conducted tests in which the angle of afterbody keel and the angle of dead rise were both investigated by the use of models developed by modifying the same basic set of lines (reference 3). The tests at Stevens Institute included both the resistance and the stability characteristics of the models.

Three angles of afterbody keel and three angles of dead rise were investigated in the present tests. The basic model of the series was considered typical of current flying boats. The variations of angle of afterbody keel included one value greater and one value smaller than that of the basic model. The angles of dead rise also included one value greater and one value smaller than the basic angle of dead rise. Nine configurations of the model, representing all possible combinations of these variations, were tested. The tests were conducted in NACA tank no. 1 during February and July 1942.

DESCRIPTION OF MODELS

The lines of the models are shown in figure 1 and the corresponding offsets are given in table I. The basic model of the series, model 126B-2, was similar to a 1/9-size model of the hull of the Navy XPB2Y-3 airplane except that the afterbody was raised to increase the depth of step, the form above the chines was simplified, and the tail turret was omitted. Models 126A-2 and 126C-2 were derived from this form by arbitrary changes in the angle of dead rise as indicated in figure 1.

The half-breadths of the chine, the width of chine flare, the height of the keel at each station, and the length of the forebody were the same for models 126A-2, 126B-2, and 126C-2. The angle between the horizontal and the straight portion of each transverse section from bow to sternpost for model 126B was 5° less than for model 126C and 5° greater than for model 126A. The radius of chine flare and the height of chine of the derived models were dependent on these established values as described in the appendix. The sections aft of the sternpost were the same for all the models.

The models were arranged with vertical wedges at the step in order that the after portion could be rotated to vary the angle of afterbody keel through the range shown in figure 1. In these variations, the depth of step and the distance from step to sternpost were held constant.

Variations in the angle of dead rise and the angle of afterbody keel for each model are given in the following table:

Model	Angle of dead rise (deg)	Angle of afterbody keel (deg)
126A-1	14¾	4
126A-2	14¾	6¼
126A-3	14¾	8½
126B-1	19	4
126B-2	19	6¼
126B-3	19	8½
126C-1	23¼	4
126C-2	23¼	6¼
126C-3	23¼	8½

APPARATUS AND PROCEDURE

The tests of each model were made by both the general method and the specific method. The NACA tank no.1 and its related equipment and the methods of the tests are described in reference 4.

The conditions of the general tests included load coefficients up to a maximum of 1.2 and speed coefficients up to 8.0. This range of loads and speeds was believed to

extend beyond all conditions at which a hull incorporating the lines of any of the models might operate. The range of trims of the models was selected to include the zero-trimming-moment condition and the best-trim condition for all the loads and speeds included.

The models were tested by the specific method at conditions corresponding to the assumed gross load and aerodynamic lift of a flying boat. The load coefficient at rest C_{Δ_o} was 1.027. The wing lift of the airplane was simulated by the use of a hydrofoil lift device that was adjusted to support the entire load of the model at a speed corresponding to the assumed value of 7.70 for the get-away speed coefficient C_{V_G}. Specific tests in the free-to-trim condition were included in the tests of the models of the 126A and 126C series. In the free-to-trim tests, the models were pivoted about an axis passing through a point corresponding to the assumed center of gravity of the flying boat. The center of gravity of each model was adjusted to the pivot point by the use of ballast located in the model and on a vertical staff above the model.

The point used as the center of gravity for the free-to-trim tests and the center of moments for the fixed-trim tests was 4.27 inches forward of the step and 16.44 inches above the keel. The pivot axis of the towing gear was located at this point in the tests of the models of the 126A and 126C series. The models of the 126B series, however, had been tested earlier with the use of additional equipment that prevented the desired location of the pivot axis. Because of this location of the pivot, no free-to-trim tests were made with the models of the 126B series. Corrections were applied to the trimming moments of the 126B series to obtain the trimming moments about the selected center of moments.

RESULTS AND DISCUSSION

Method of Presenting Data

Nondimensional coefficients based on Froude's law were used to present the results of the tests. The nondimensional coefficients are defined as follows:

C_V speed coefficient $(V/\sqrt{gb})$

C_Δ load coefficient (Δ/wb^3)

C_M trimming-moment coefficient (M/wb^4)

C_R resistance coefficient (R/wb^3)

where

b beam at step, feet

V speed, feet per second

Δ load on water, pounds

M trimming moment, pound-feet

w specific weight of water, pounds per cubic foot (63.5 for these tests: usually taken as 64.0 for sea water)

R resistance, pounds

g acceleration of gravity (32.2 ft/sec^2)

The moments are referred to a point 4.28 inches forward of the step and 16.44 inches above the base line. Moments having a tendency to raise the bow are considered positive. Trim is the angle between the base line and the horizontal.

Free-to-Trim Tests

The effects on resistance coefficient, trim, and load-resistance ratio of angle of afterbody keel and of angle of dead rise are given in figures 2 and 3, respectively. The curves for the models of the 126A and 126C series in figures 2(a) and 2(c) were plotted from the free-to-trim tests of the models. The curves for the 126B series in figure 2(b) were derived from cross plots of the data from the fixed-trim specific tests of the models.

The effect of angle of afterbody keel upon the free-to-trim characteristics for angles of dead rise of $14\frac{3}{4}^\circ$, 19°, and $23\frac{1}{4}^\circ$ may be seen by comparisons of the curves of

figures 2(a), 2(b), and 2(c). Reducing the angle of dead rise reduced the trim and the resistance at all speeds up to and including the hump. The effect of increasing the angle of afterbody keel was opposite and of about the same order of magnitude. At speeds in excess of the hump speed, the effect of the angle of afterbody keel became less and, at equal angles of dead rise, the trim and the resistance of the models became approximately equal after the afterbodies came clear of the water. The effects of changing the angle of afterbody keel were substantially the same for the models of different dead rise except that the differences in trim and resistance persisted at higher speeds for models of greater dead rise.

The effects of angle of dead rise on models of equal angle of afterbody keel may be seen by a comparison of the free-to-trim curves of models 126A-2, 126B-2, and 126C-2. in figure 3. The changes in angle of dead rise caused relatively small changes in the resistance at the hump. Lower angles of dead rise resulted in increased trim at the hump and decreased trim at speed coefficients above 4.0. This effect on the trim at higher speeds may account for the fact that the effects of angle of afterbody keel extended to higher speeds for the models with greater values of angle of dead rise.

General Tests

The variation with speed coefficient of best trim, resistance coefficient at best trim, and trimming-moment coefficient at best trim, derived from the data obtained in the general tests, is given in figures 4 to 6 for the models of the 126A series, the 126B series, and the 126C series, respectively. Resistance coefficient and trimming-moment coefficient plotted against trim are shown in figure 7 to provide direct comparisons of the results of the general tests. Comparisons of the curves in any of the three groups of figure 7(a) show that, at hump speed, decreasing the angle of afterbody keel reduced the resistance at all trims, reduced the best trim, and reduced the values of the positive trimming moments. Changes of angle of afterbody keel caused approximately the same effects when applied to models of any angle of dead rise included in the investigation. At a speed coefficient of 4.5 (fig. 7(b)), the effect of angle of afterbody keel upon resistance coefficient was negligible. At this speed the afterbody was clear of the water at most trims. The curves of trimming-

moment coefficient in figure 7(b) show some effect from the contact of the afterbody with the water at high trims. This effect was more pronounced in the case of the models with greater angles of dead rise. The curves of resistance coefficient and trimming-moment coefficient at speeds near get-away, $C_V = 6.0$ and $C_V = 7.0$, are shown in figures 7(c) and 7(d), respectively. At high speeds the effect of angle of afterbody keel was so small that the scatter of the experimental data caused some obvious reversals in the comparative results. This scatter of data was caused in part by the changes in wind velocity that resulted from openings in the wall of the building. It is believed, however, that the qualitative effects of the changes of the models are conclusively shown by the curves. At this condition high angles of afterbody keel gave the most favorable resistance characteristics. Smaller angles of afterbody keel caused no change in the resistance at extremely low trims but caused increases in resistance that started at approximately best trim and became larger as the trim was increased.

The lowest angle of dead rise investigated gave the lowest resistance at the hump and at all speeds above the hump (fig. 7). Throughout this range of speed the resistance was increased slightly by each increase in the angle of dead rise. This effect was consistent for each angle of afterbody keel that was investigated. A comparison of the curves of trimming-moment coefficient in figure 7(b) shows that the action of the afterbody was influenced to some extent by variations of the angle of dead rise. At this condition the effect of angle of afterbody keel became more pronounced as the angle of dead rise was increased. This relationship between the effects of angle of afterbody keel and angle of dead rise was in agreement with that observed in the results of the free-to-trim tests (fig. 2).

Spray Characteristics

Photographs taken during the fixed-trim specific tests of the models are reproduced as figures 8 to 11. The conditions selected for the comparisons, 11° trim at hump speed and 5° trim at a higher speed, $C_V = 5.0$, correspond approximately to conditions at which flying boats incorporating these lines might operate.

The effects on spray of angle of afterbody keel at

hump speed and at planing speed are shown in figures 8 and 9, respectively. In the fixed-trim condition at the hump speed, the lower angles of afterbody keel resulted in slightly lower spray from the forebody and considerably more spray from the afterbody and the tail extension. The spray around the tails should be disregarded in this comparison because the tail extension of the model was moved with the afterbody when the angle of afterbody keel was changed. At higher speed (fig. 9), the lowest angle of afterbody keel caused the spray to strike the bottom of the afterbody. This effect became more pronounced at speeds near get-away.

The effects on spray of angle of dead rise at hump speed and at planing speed are shown in figures 10 and 11, respectively. The height of the spray decreased as the angle of dead rise increased. This effect is shown at the conditions of both figures 10 and 11 and was observed throughout the range of speeds investigated. At extremely low speeds, the bows of the models with low dead rise were much dirtier than those with higher dead rise. The stern views in figure 10 show that, at an angle of dead rise of $23\frac{1}{2}^{\circ}$, the afterbody of model 126C-3 was in the water at test conditions at which the afterbodies of the models of lower dead rise were clear of the water.

Working Charts for Model 126B-2

Inasmuch as any change in angle of afterbody keel or angle of dead rise will cause both favorable and unfavorable effects upon the performance of the model, the selection of an optimum angle of dead rise or an optimum angle of afterbody keel is difficult if not impossible. It is possible that the angle of dead rise or the angle of afterbody keel selected for a flying boat might depend to a large extent upon other characteristics peculiar to the design or upon the operating conditions that are anticipated. The results of the tests, however, have shown that model 126B-2 represents a fair compromise of the two angles investigated. Because of this fact and because model 126B-2 is more representative of current practice, working charts derived from the general tests of this model are given in figure 12. The derivation and the use of the charts are described in detail in reference 5.

CONCLUSIONS

The results of the present investigation were in agreement with the results of previous research on the effects of angle of afterbody keel and angle of dead rise. Because of the large number of configurations tested and the agreement with the results of other tests of varied types of model, it is believed that the following general conclusions may be drawn from the results of the present tests:

1. At practicable angles of dead rise, increasing the angle of afterbody keel increased the resistance at low speeds and at the hump, reduced the resistance at high speeds, increased the best trim, and increased the trim in the free-to-trim condition.

2. Increasing the angle of dead rise in the normal range for V-bottom hulls increased the resistance at the hump and at higher speeds and reduced the height of spray.

It was also observed in the present tests that larger angles of dead rise caused the afterbody to remain in the water at higher speeds.

Langley Memorial Aeronautical Laboratory,
National Advisory Committee for Aeronautics,
Langley Field, Va.

APPENDIX

DERIVATION OF STATIONS OF MODELS 126A AND 126C FROM MODEL 126B

From figure 13, the angle of dead rise of the straight portion and the breadth of the chine flare at each station of the forebody of model 126B are obtained from the expressions

$$\theta_o = \tan^{-1}\frac{B}{A}$$

$$X = R_1 \sin \theta$$

Then, for the corresponding station of the derived models, for model 126A,

$$\theta = \theta_o - 5^\circ$$

for model 126C,

$$\theta = \theta_o + 5^\circ$$

$$B = A \tan \theta$$

where A is the same as for model 126B,

$$R_1 = X/\sin \theta$$

where X is the same as for model 126B,

$$Y = (A - X) \tan \theta$$

and

$$E = Y + R_1(1 - \cos \theta)$$

The height of chine of the afterbody is obtained from the expression

$$B = F \tan \theta$$

where F is the same as for model 126B.

REFERENCES

1. Allison, John M.: The Effect of the Angle of After-body Keel on the Water Performance of a Flying-Boat Hull Model. T.N. No. 541, NACA, 1935.

2. Parkinson, John B., Olson, Roland E., and House, Rufus O.: Hydrodynamic and Aerodynamic Tests of a Family of Models of Seaplane Floats with Varying Angles of Dead Rise. N.A.C.A. Models 57-A, 57-B, and 57-C. T.N. No. 716, NACA, 1939.

3. Davidson, Kenneth S. M., and Locke, F. W. S., Jr.: Some Systematic Model Experiments on the Porpoising Characteristics of Flying Boat Hulls. NACA ARR No. 3F12, 1943.

4. Truscott, Starr: The Enlarged N.A.C.A. Tank, and Some of Its Work. T.M. No. 918, NACA, 1939.

5. Dawson, John R.: A General Tank Test of a Model of the Hull of the P3M-1 Flying Boat Including a Special Working Chart for the Determination of Hull Performance. T.N. No. 681, NACA, 1938.

TABLE I. - OFFSETS FOR NACA MODEL 126 SERIES

[All values given in in.]

Station	Distance from forward perpendicular	All models								Model 126A			Model 126B			Model 126C		
		A	C	F	G	H	J	R_2	R_3	B	E	R_1	B	E	R_1	B	E	R_1
Forward perpendicular	0		14.33															
0.1	3.00	2.09	6.06							1.27	0.94	1.98	1.54	1.12	1.74	1.84	1.32	1.56
.2	4.75	3.43	4.06							2.61	2.07	2.11	3.12	2.44	1.90	3.71	2.89	1.74
1.0	6.50	4.26	2.69							3.28	2.67	2.33	3.91	3.16	2.10	4.66	3.73	1.92
1.1	8.98	5.08	1.52							3.66	3.02	2.75	4.38	3.59	2.47	5.22	4.24	2.25
1.2	11.46	5.68	.95							3.59	2.97	3.41	4.32	3.55	3.00	5.17	4.22	2.71
1.3	13.94	6.19	.68							3.29	2.71	4.37	4.02	3.30	3.77	4.83	3.94	3.33
2.0	16.42	6.57	.54							3.00	2.47	5.37	3.72	3.06	4.52	4.52	3.68	3.93
2.2	21.61	6.96	.34							2.54	2.10	6.87	3.26	2.68	5.57	4.03	3.29	4.71
2.4	26.81	7.00	.25							2.27	1.88	7.50	2.96	2.45	5.93	3.71	3.06	4.93
3.1	32.07	7.00	.16							2.21	1.84	7.55	2.90	2.41	5.93	3.64	3.01	4.91
3.3	37.40	7.00	.07							2.21	1.84	7.55	2.90	2.41	5.93	3.64	3.01	4.91
[a]3.5 F	41.49	7.00	0							2.21	1.84	7.55	2.90	2.41	5.93	3.64	3.01	4.91
A	41.49	7.00	.70	7.00						2.21			2.90			3.64		
4.1	46.25	6.92	1.22	6.92						2.18			2.87			3.60		
4.3	50.94	6.63	1.73	6.49	3.23	1.10	2.83	4.00	1.11	2.05			2.69			3.38		
5.1	55.62	6.32	2.24	5.77	3.08	1.60	3.85	3.79	1.11	1.82			2.39			3.00		
5.3	60.31	6.01	2.76	4.74	2.93	2.11	4.87	3.59	1.11	1.49			1.96			2.47		
6.0	65.00	5.70	3.27	3.40	2.78	2.61	5.88	3.38	1.11	1.07			1.41			1.77		
6.2	70.00	5.37	3.82	1.40	2.62	3.15	6.97	3.16	1.11	.44			.58			.73		
7.0	72.50	5.21	4.10	.10	2.54	3.42	7.51	3.05	1.11	.03			.04			.05		

[a] F indicates forebody; A, afterbody.

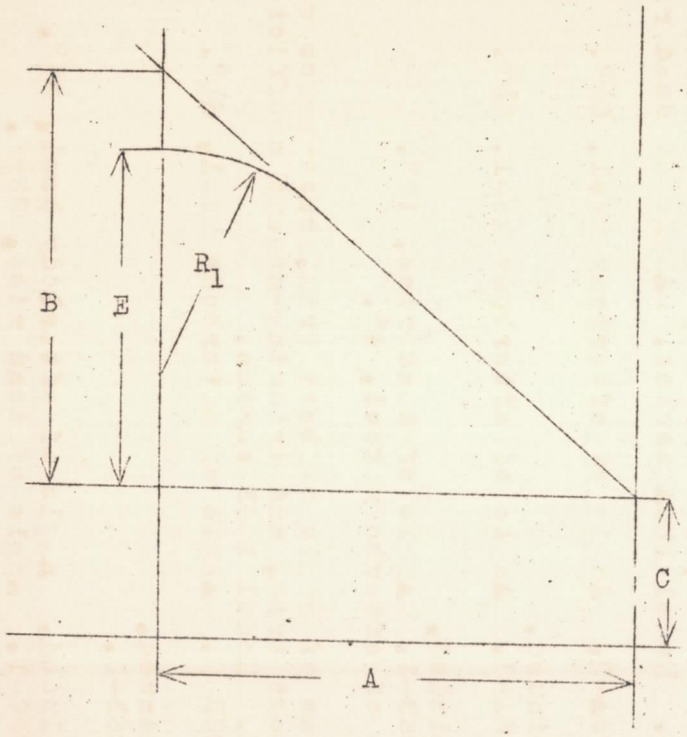

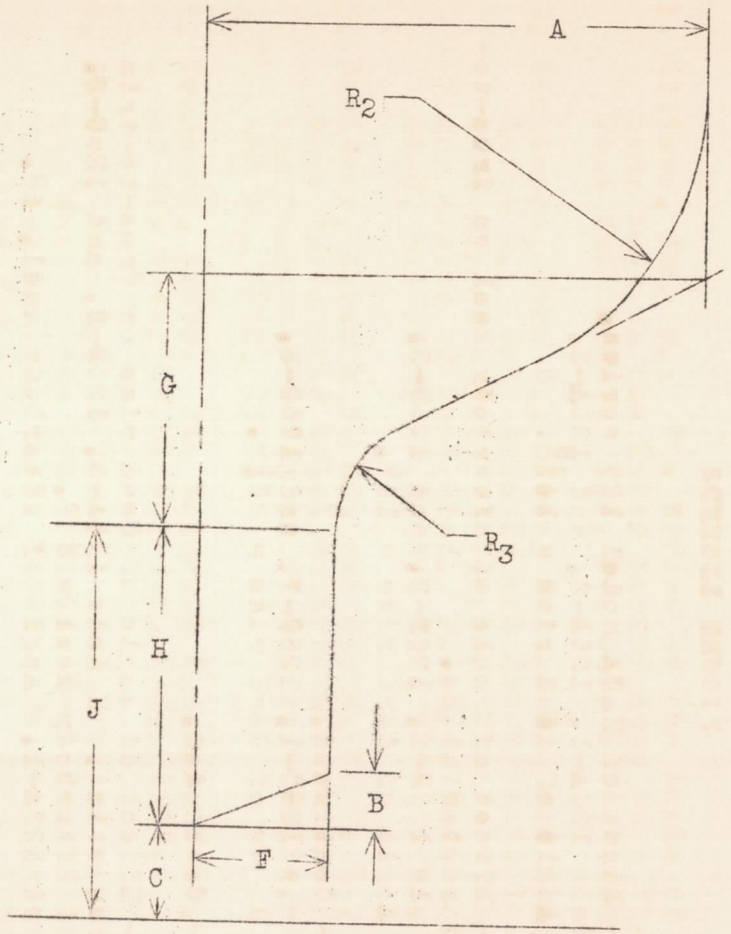

Model	Height of chine at bow
126A	7.19
126B	7.33
126C	7.47

Diagram for Table I.

FIGURE LEGENDS

Figure 1.– Lines of NACA model 126 series.
(a) Models 126A–1, 126A–2, and 126A–3.
Angle of dead rise = $14\frac{3}{4}^{\circ}$.

Figure 2.– Effect of angle of afterbody keel on free-to-trim characteristics.
(b) Models 126B–1, 126B–2, and 126B–3.
Angle of dead rise = 19°.

Figure 2.– Continued.
(c) Models 126C–1, 126C–2, and 126C–3.
Angle of dead rise = $23\frac{1}{4}^{\circ}$.

Figure 2.– Concluded.

Figure 3.– Effect of angle of dead rise on free-to-trim characteristics. Models 126A–2, 126B–2, and 126C–2.
Angle of afterbody keel = $6\frac{1}{2}^{\circ}$.
(a) Model 126A–1. Angle of afterbody keel, 4°.

Figure 4.– Curves of angle of best trim, resistance coefficient at best trim, and trimming-moment coefficient at best trim. Model 126A series. Angle of dead rise, $14\frac{3}{4}^{\circ}$.
(b) Model 126A–2. Angle of afterbody keel, $6\frac{1}{2}^{\circ}$.

Figure 4.– Continued.
(c) Model 126A–3. Angle of afterbody keel, $8\frac{1}{2}^{\circ}$.

Figure 4.– Concluded.
(a) Model 126B–1. Angle of dead rise, 19°.
Angle of afterbody keel, 4°.

Figure 5.– Curves of angle of best trim, resistance coefficient at best trim, and trimming-moment coefficient at best trim. Model 126B series.
(b) Model 126B–2. Angle of afterbody keel, $6\frac{1}{2}^{\circ}$.

Figure 5.– Continued.
(c) Model 126B–3.

Figure 5.– Concluded. Angle of afterbody keel, $8\frac{1}{2}^{\circ}$.
(a) Model 126C–1. Angle of dead rise, $23\frac{1}{4}^{\circ}$.
Angle of afterbody keel, 4°.

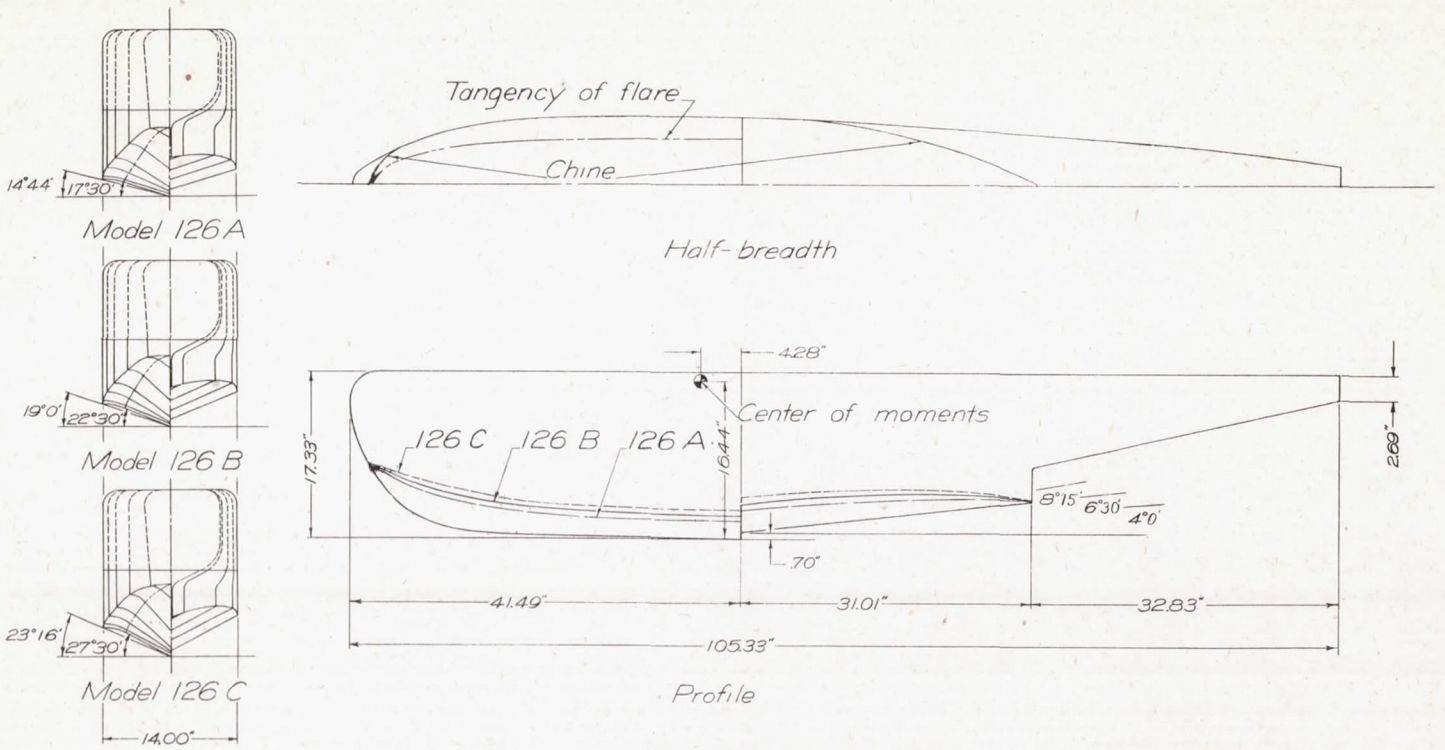

Figure 1.— Lines of NACA model 126 series.

L-305

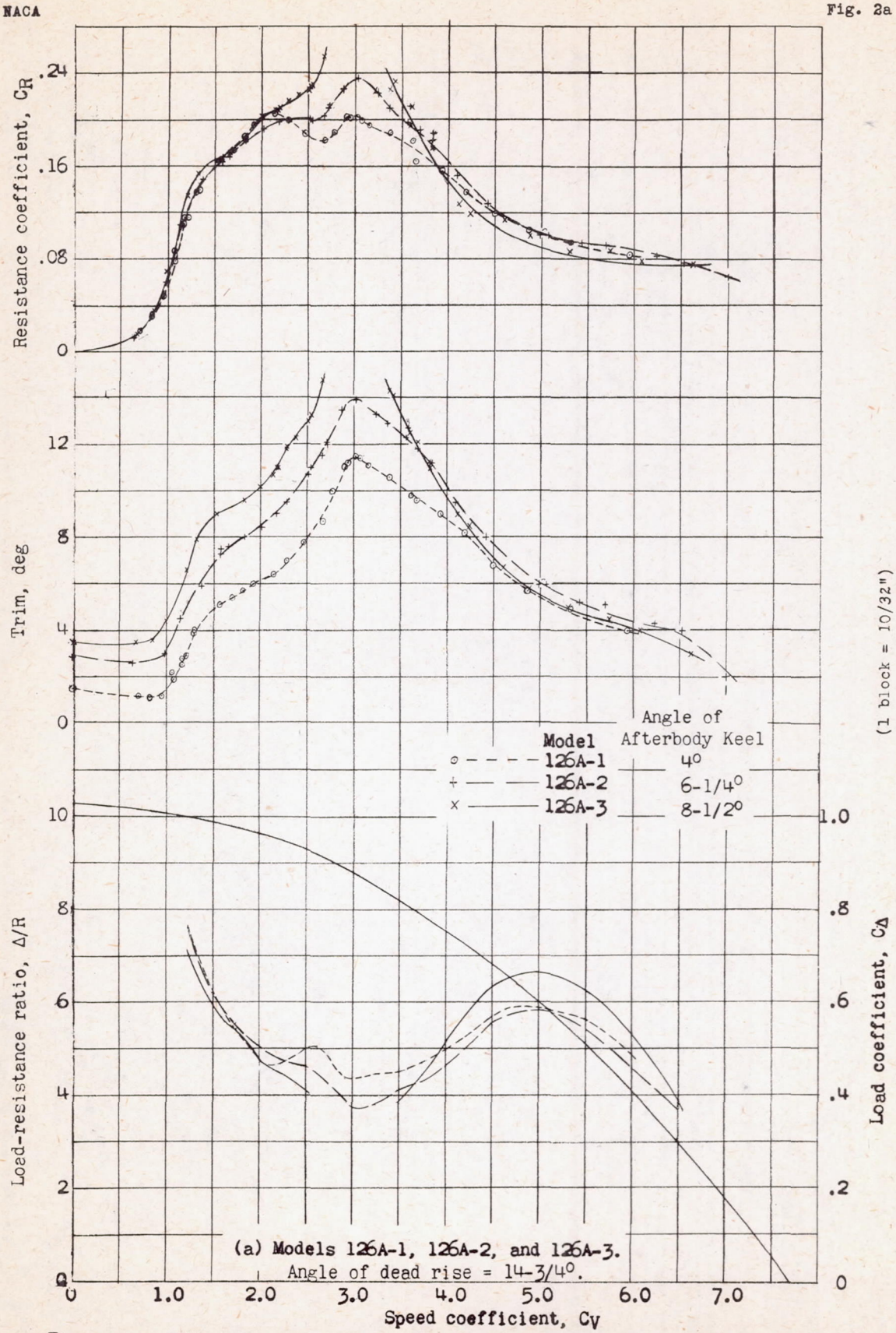

Figure 2. - Effect of angle of afterbody keel on free-to-trim characteristics.

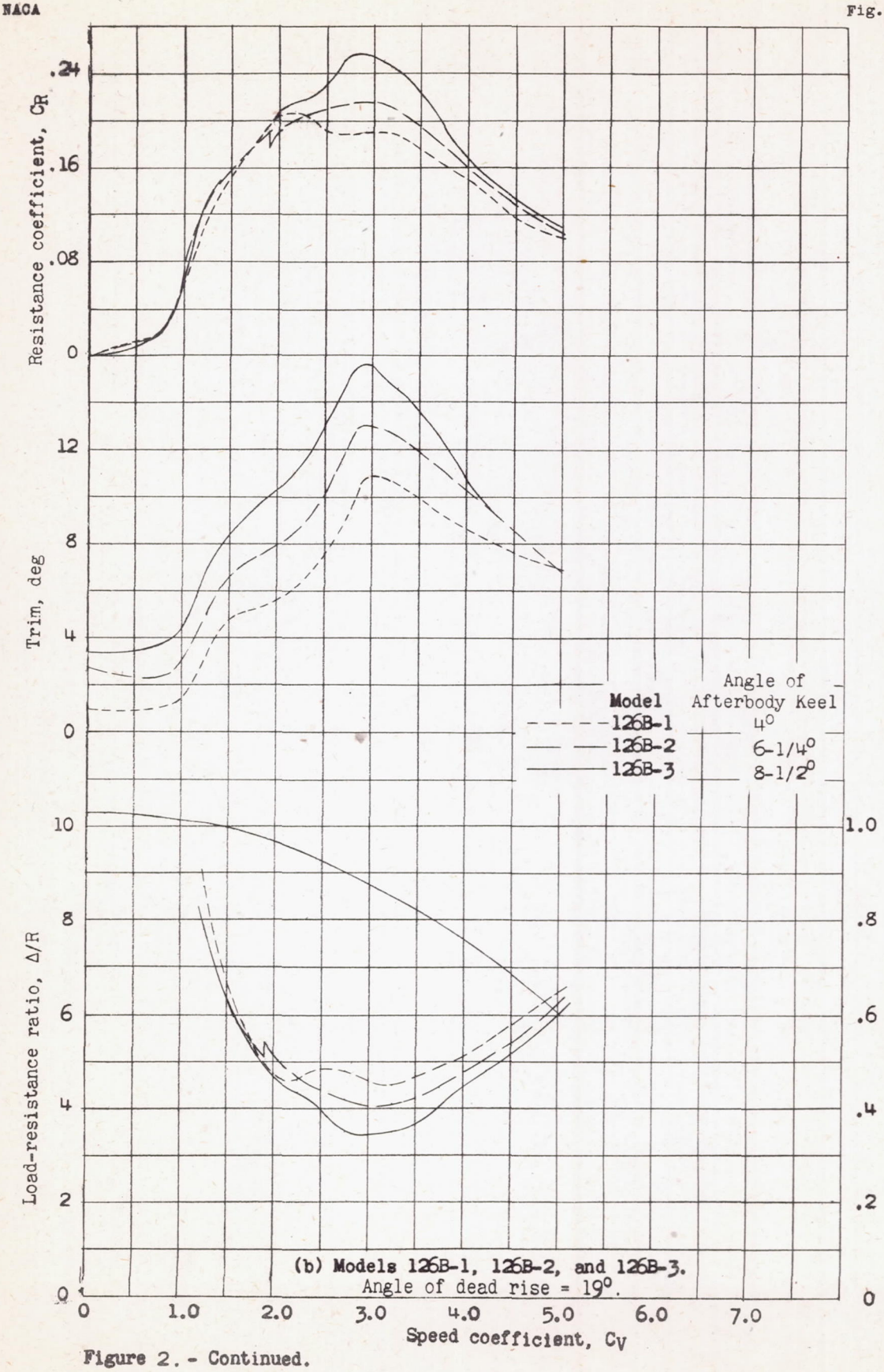

(b) Models 126B-1, 126B-2, and 126B-3.
Angle of dead rise = 19°.

Figure 2. - Continued.

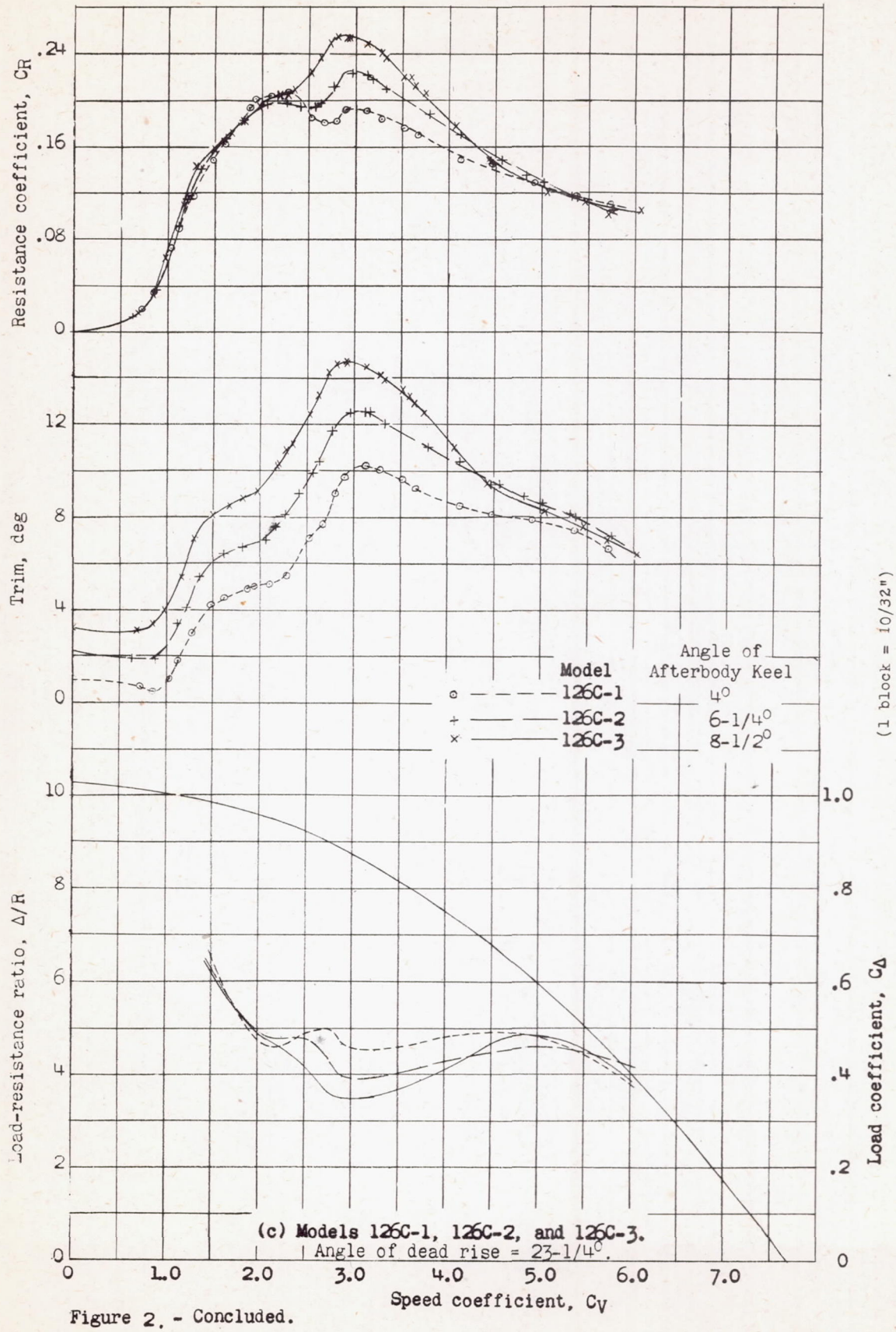

(c) Models 126C-1, 126C-2, and 126C-3.
Angle of dead rise = 23-1/4°.

Figure 2. - Concluded.

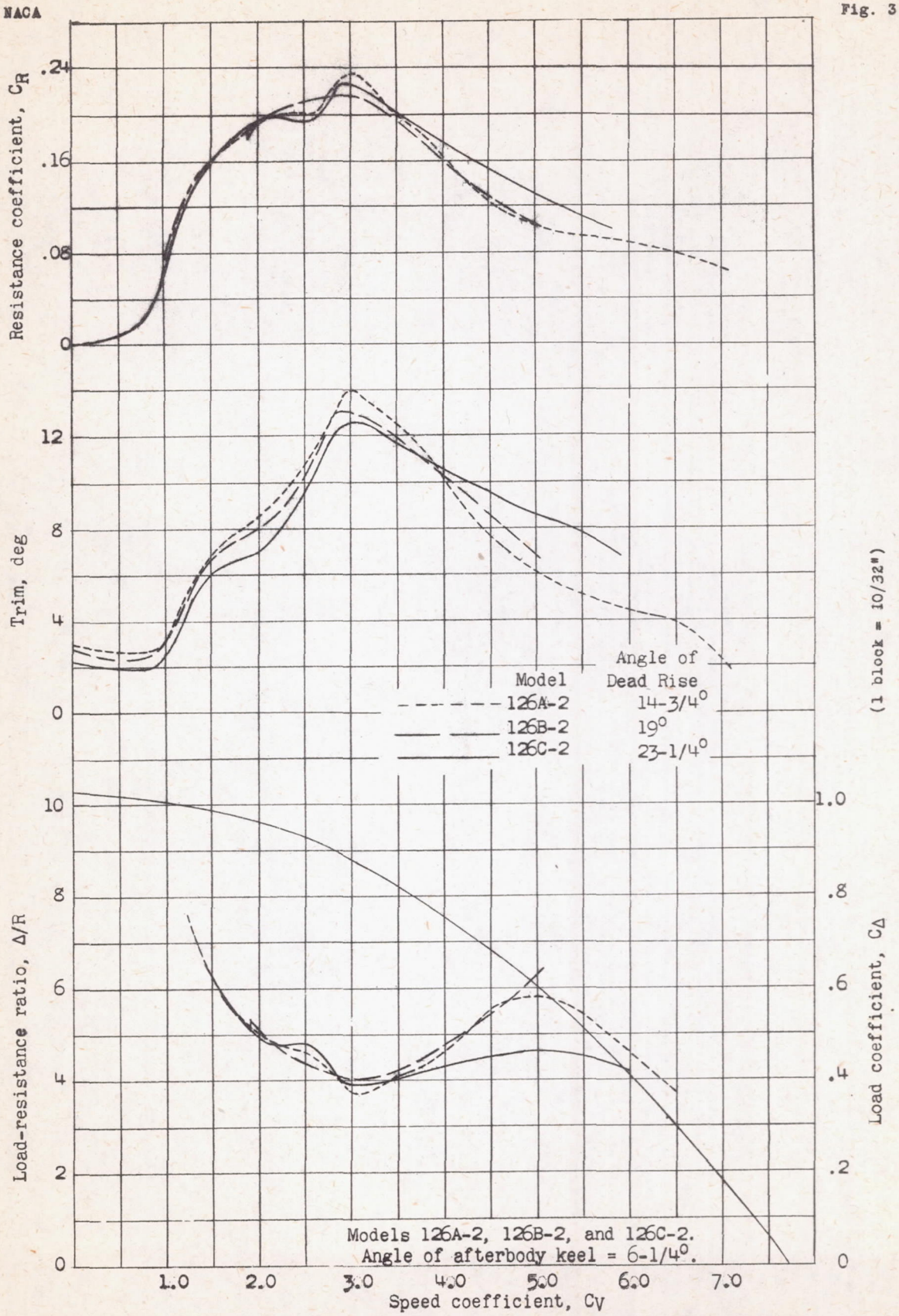

Figure 3 .- Effect of angle of dead rise on free-to-trim characteristics.

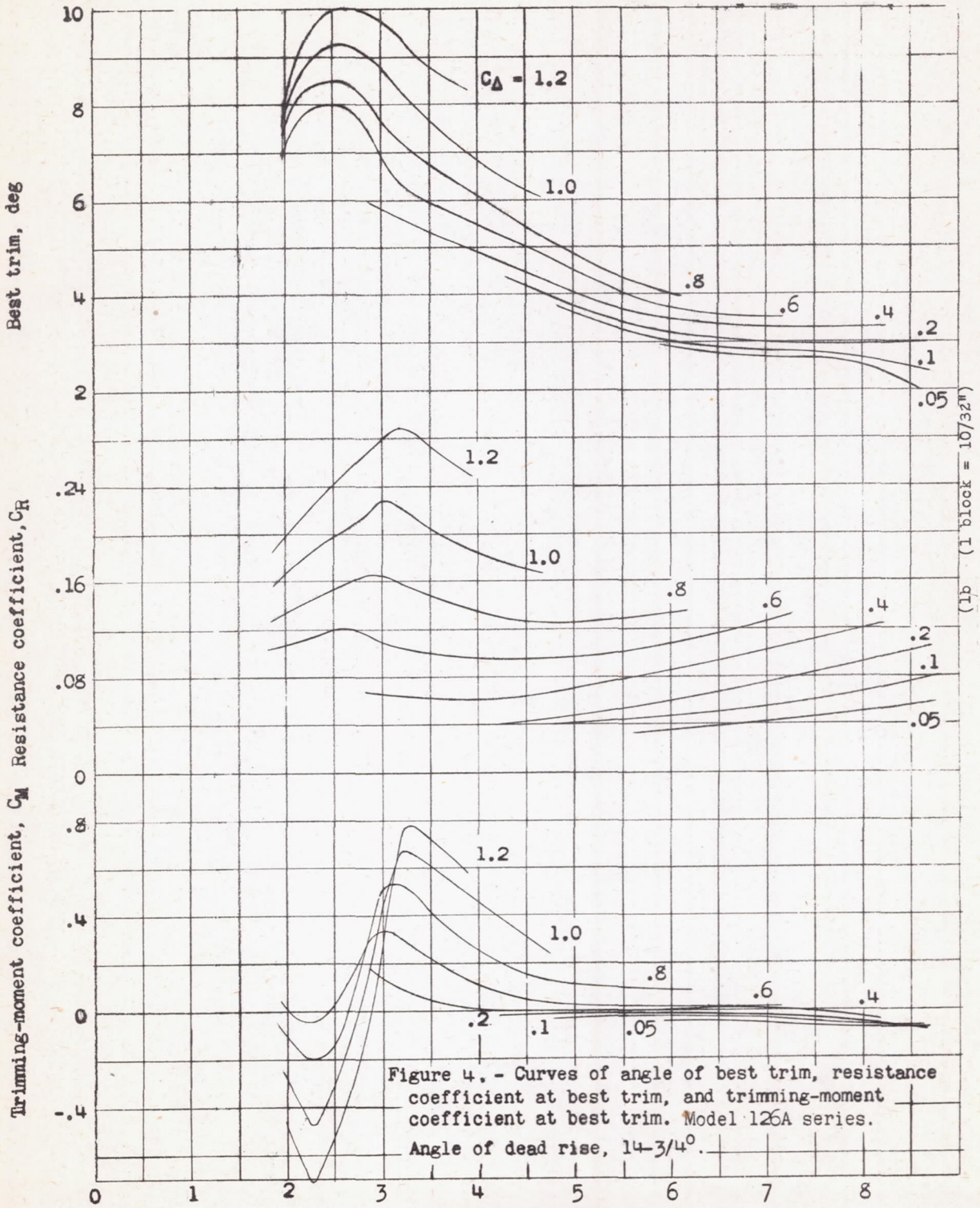

Figure 4. - Curves of angle of best trim, resistance coefficient at best trim, and trimming-moment coefficient at best trim. Model 126A series.

Angle of dead rise, 14-3/4°.

(a) Model 126A-1. Angle of afterbody keel, 4°.

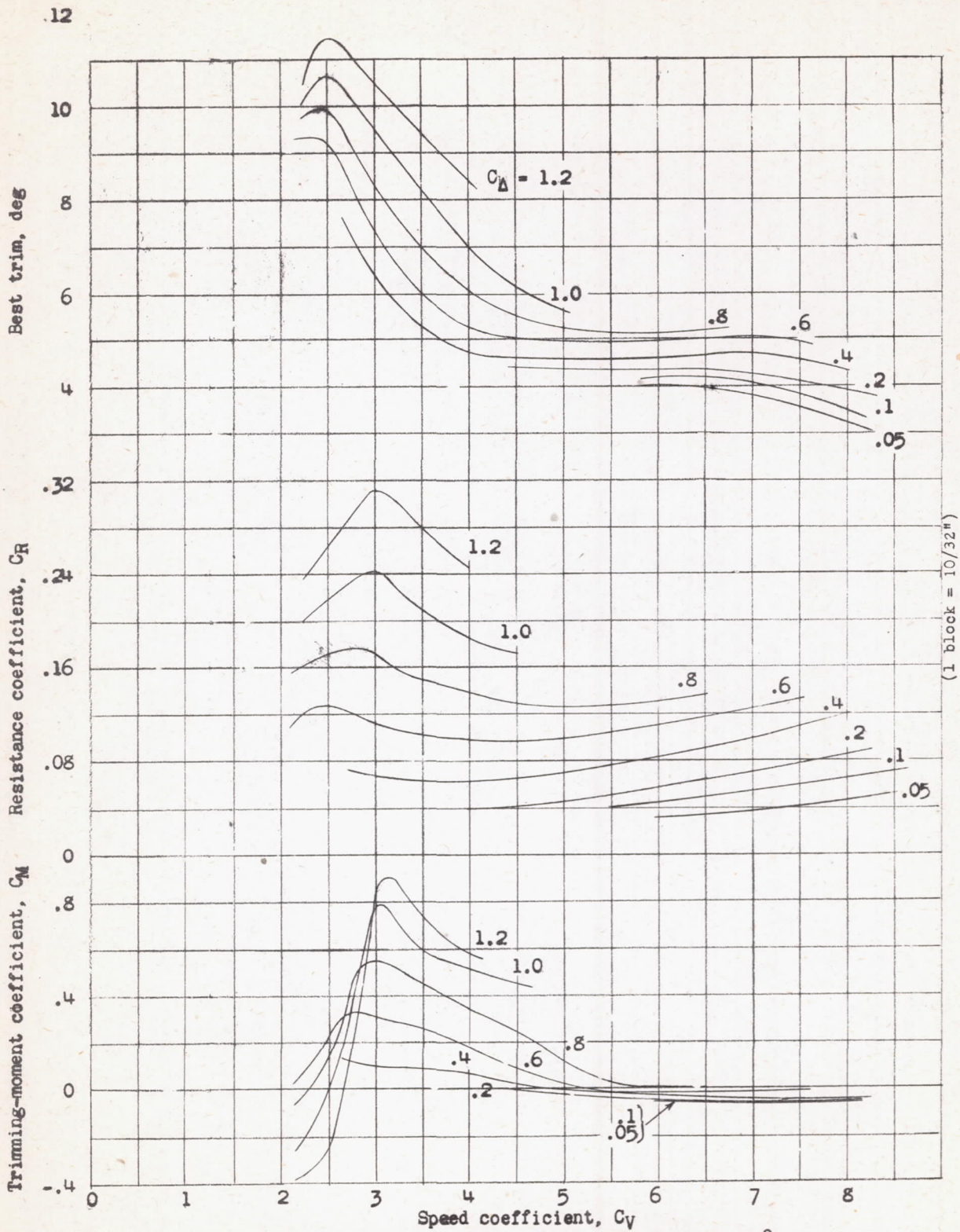

(b) Model 126A-2. Angle of afterbody keel, 6-1/4°.

Figure 4. - Continued.

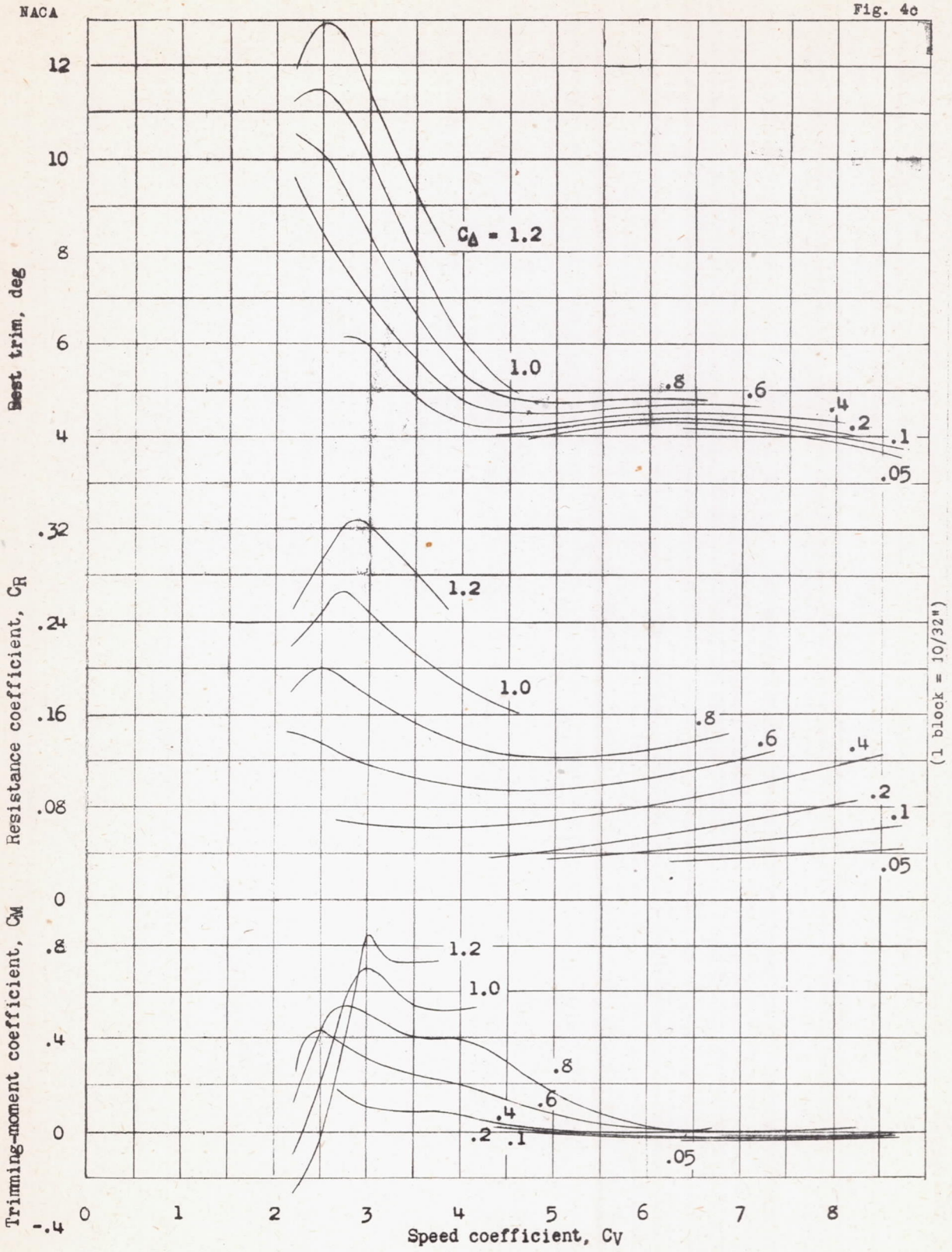

(c) Model 126A-3. Angle of afterbody keel, 8-1/2°.

Figure 4. - Concluded.

L-305

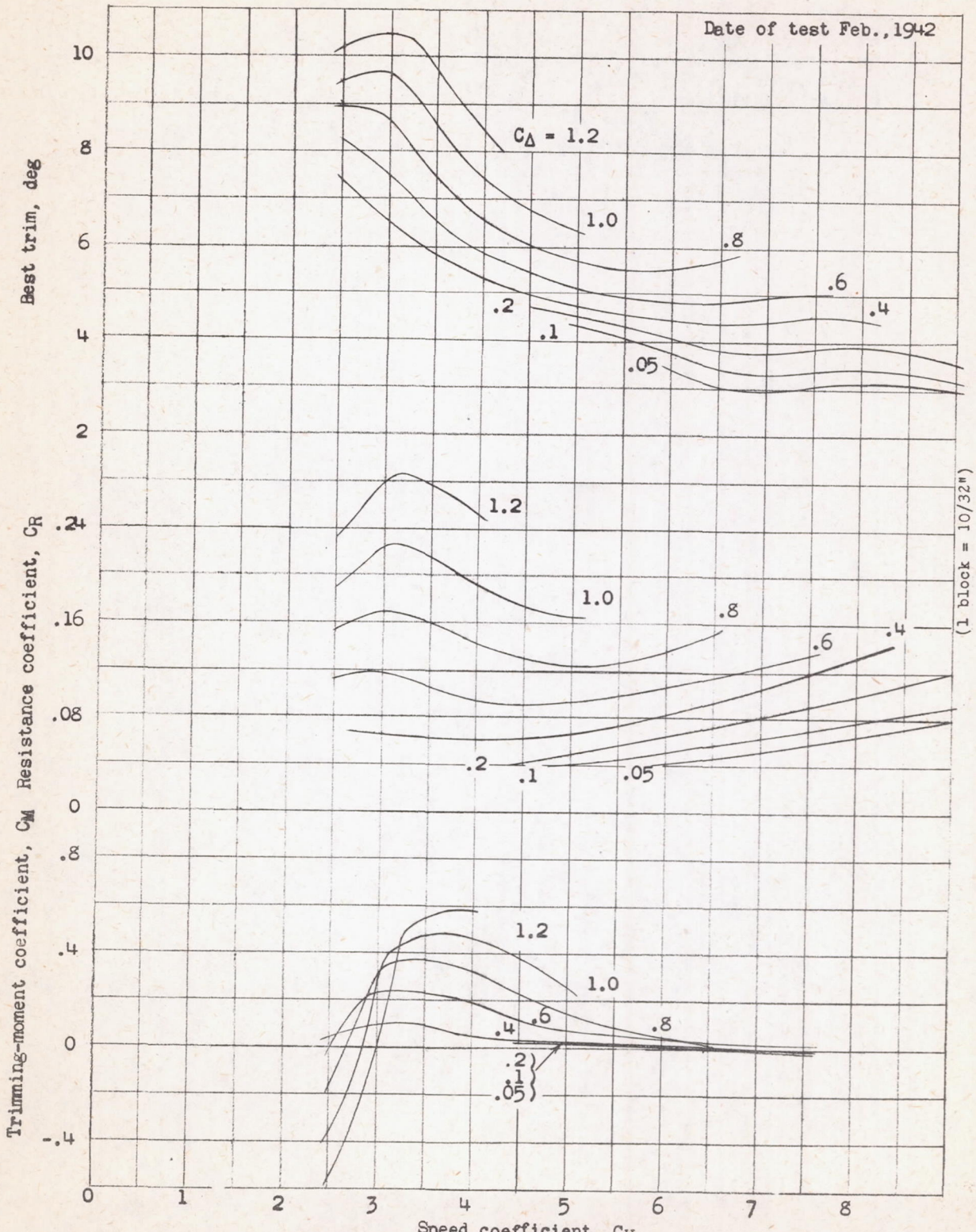

(a) Model 126B-1. Angle of dead rise, 19°. Angle of afterbody keel, 4°.

Figure 5.- Curves of angle of best trim, resistance coefficient at best trim, and trimming-moment coefficient at best trim. Model 126B series.

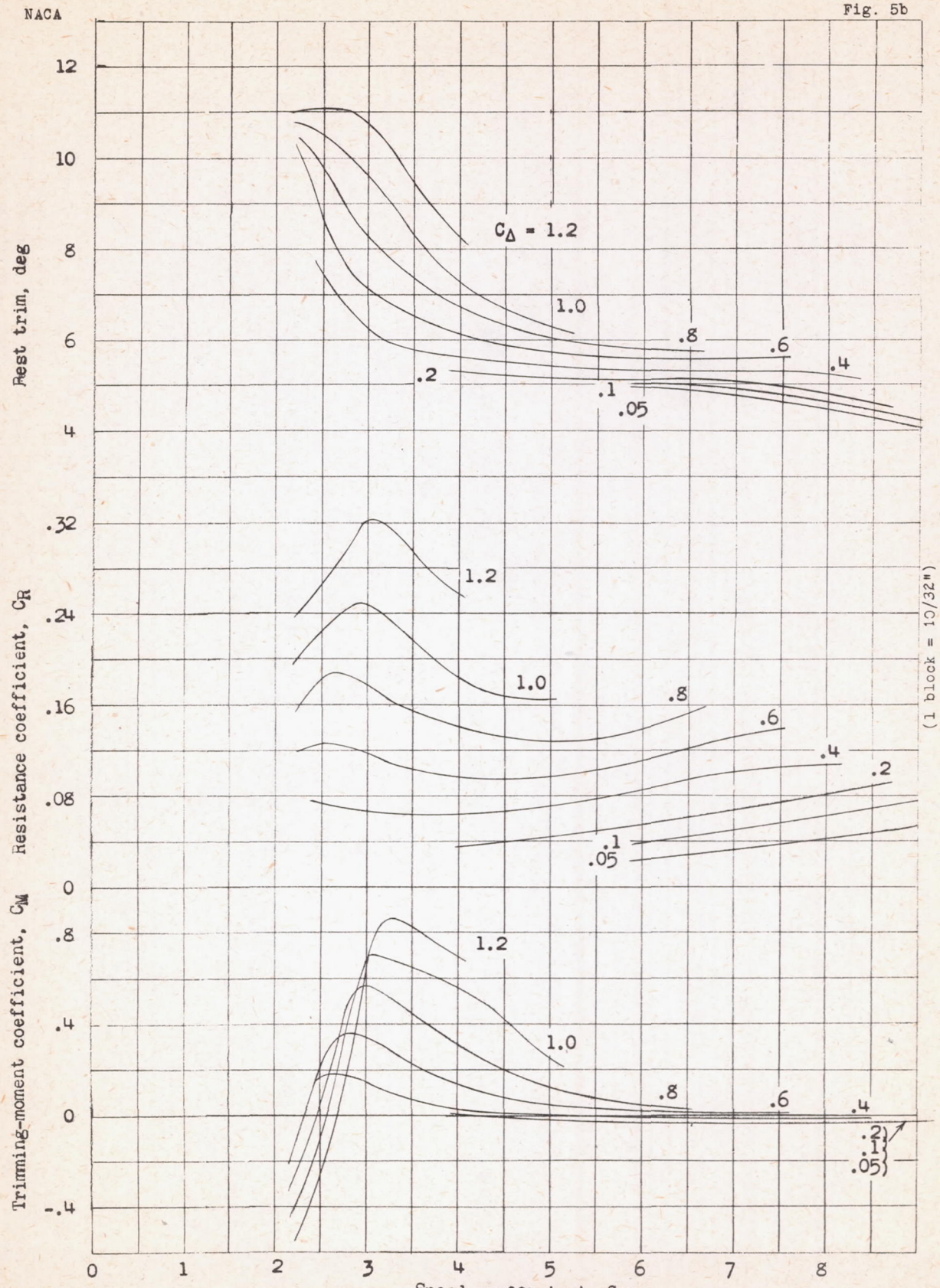

(b) Model 126B-2. Angle of afterbody keel, 6-1/4°.

Figure 5. - Continued.

L-305

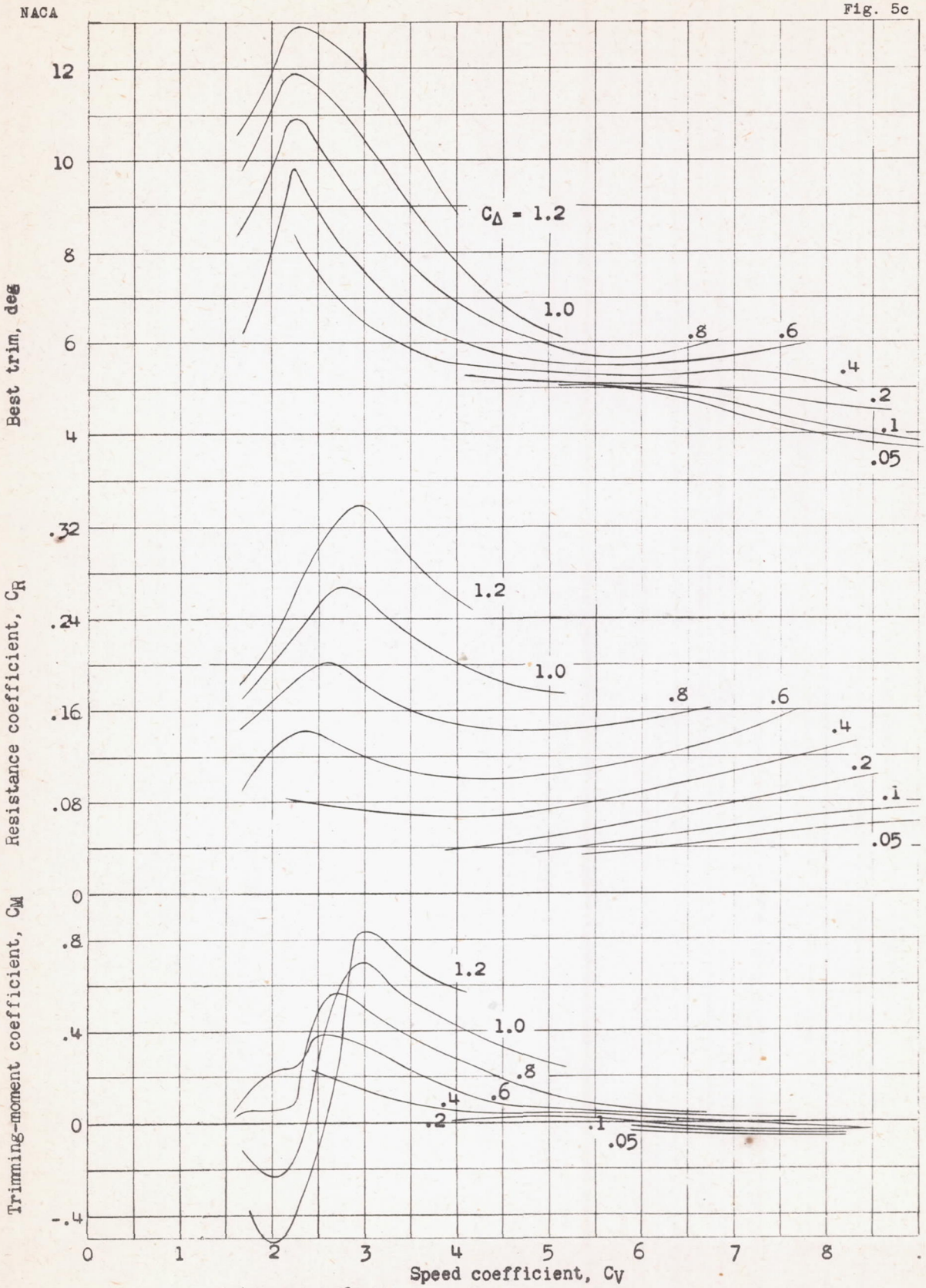

(c) Model 126B-3.

Figure 5.- Concluded. Angle of afterbody keel, 8-1/2°.

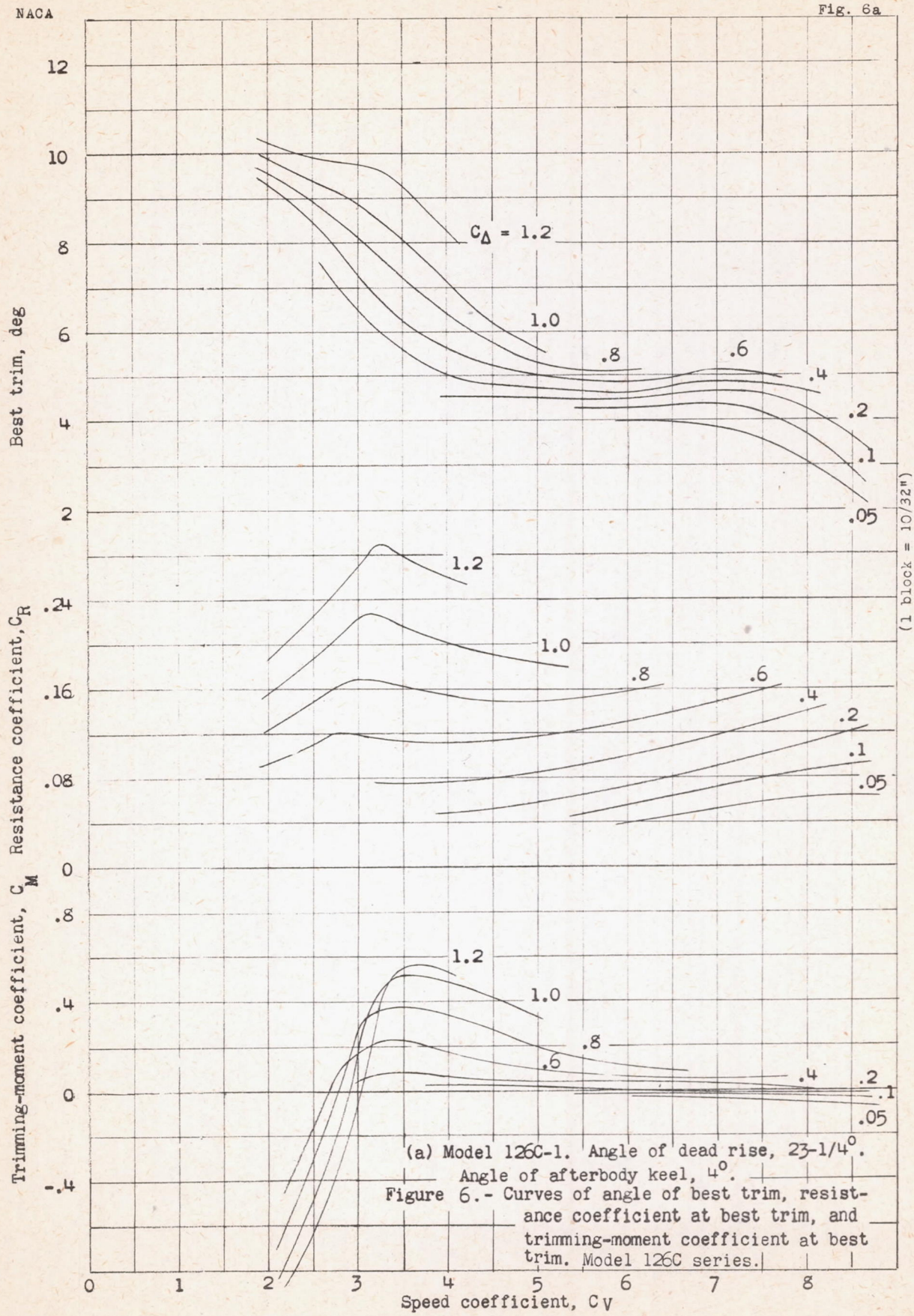

(a) Model 126C-1. Angle of dead rise, 23-1/4°. Angle of afterbody keel, 4°.

Figure 6.- Curves of angle of best trim, resistance coefficient at best trim, and trimming-moment coefficient at best trim. Model 126C series.

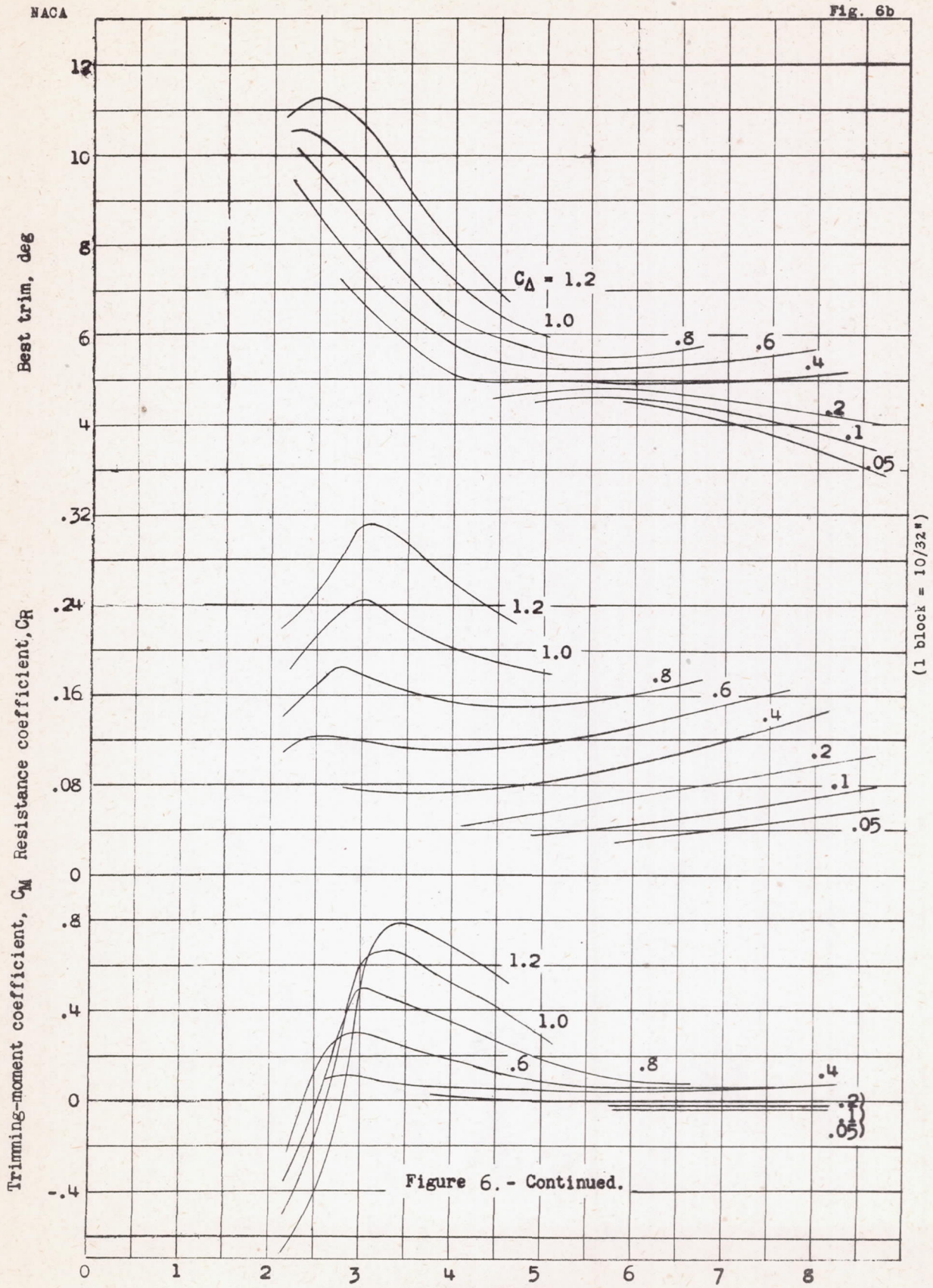

Figure 6. - Continued.

(b) Model 126C-2. Angle of afterbody keel, 6-1/4°.

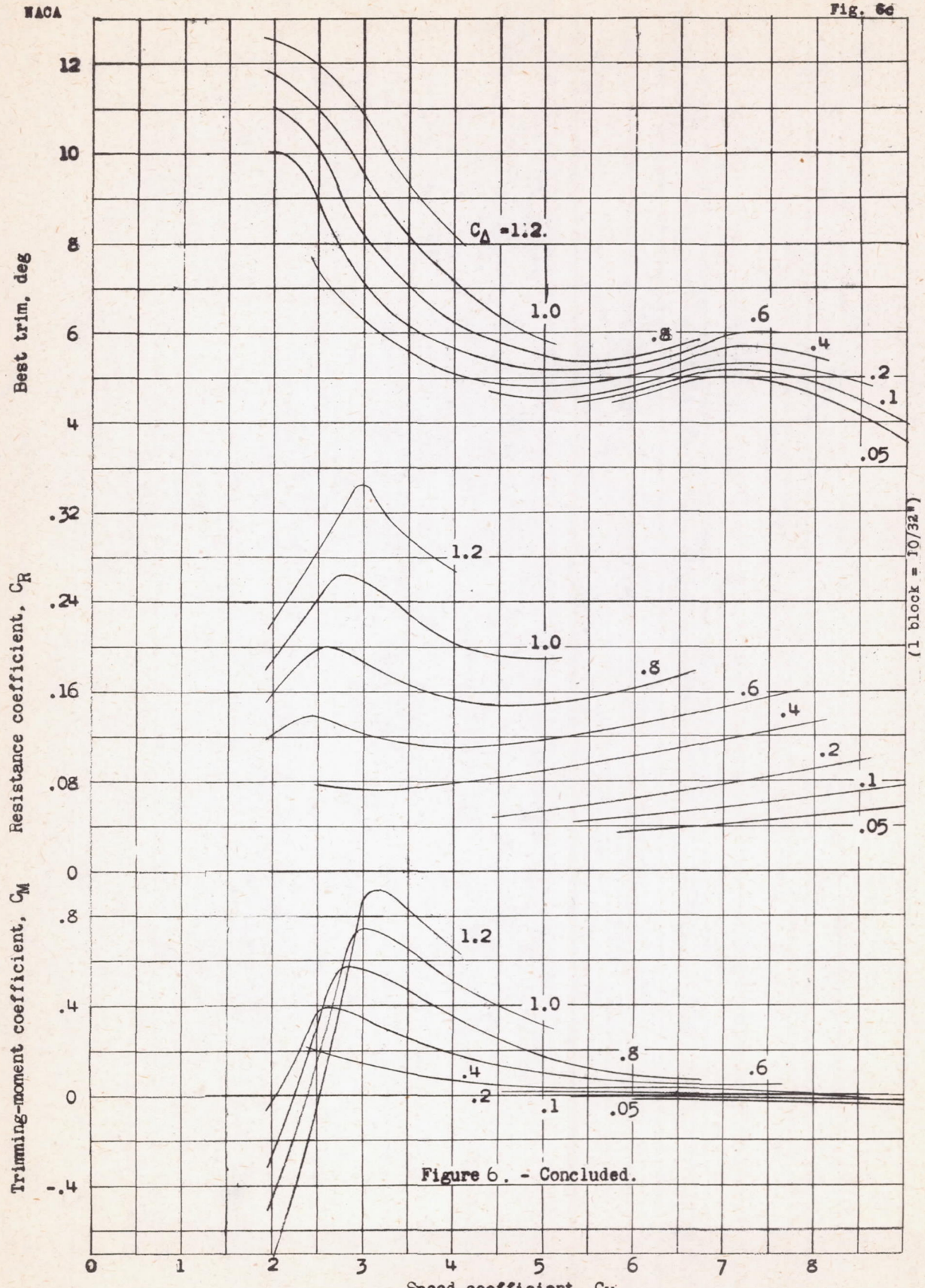

Figure 6. - Concluded.

c) Model 126C-3. Angle of afterbody keel, 8-1/2°.

NACA

Fig. 7a

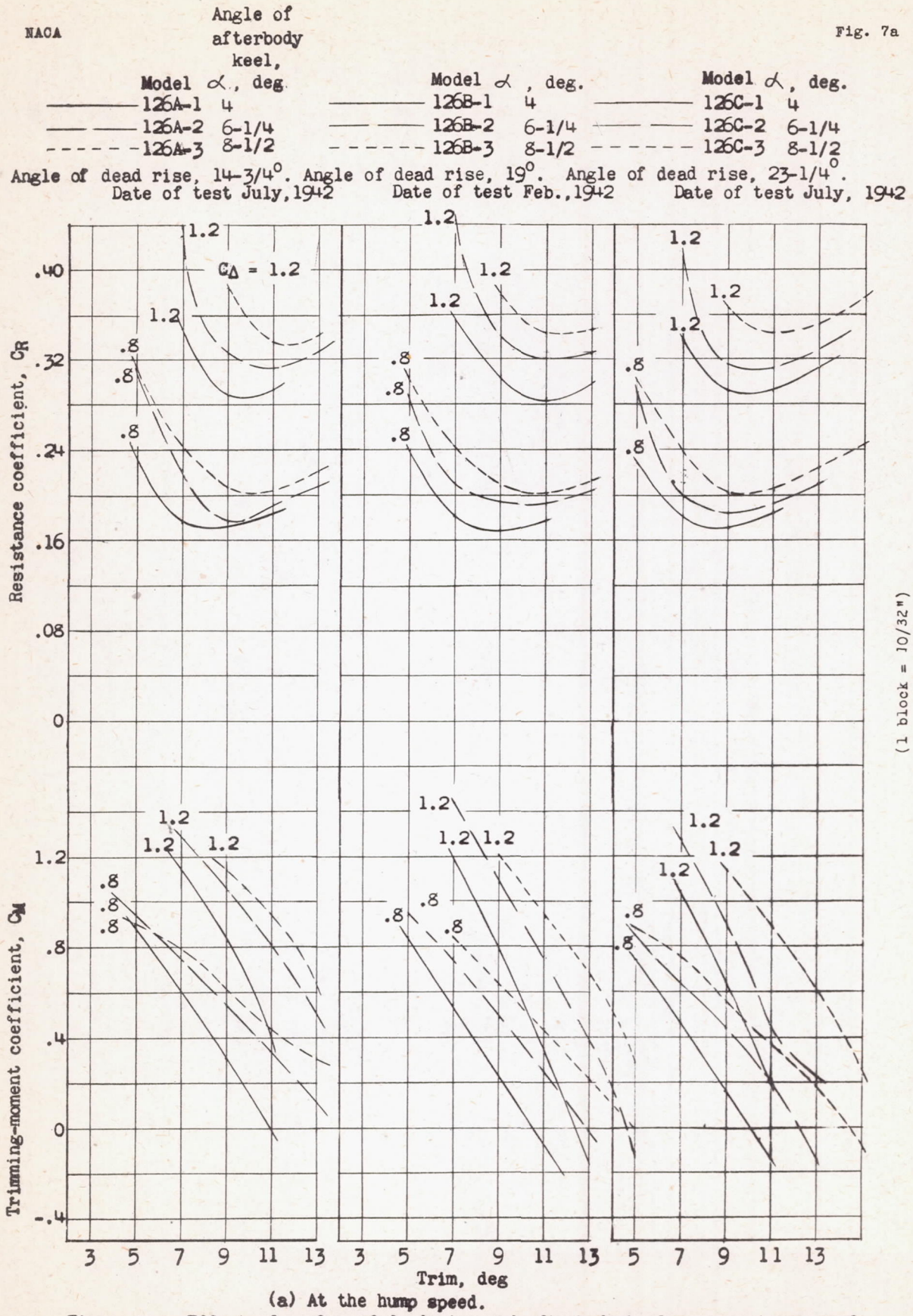

(a) At the hump speed.

Figure 7. - Effect of angles of dead rise and afterbody keel on resistance coefficient and trimming-moment coefficient.

NACA

Fig. 7b

Model	Angle of afterbody keel, α, deg.
126A-1	4
126A-2	6-1/4
126A-3	8-1/2

Angle of dead rise, 14-3/4°. Date of test July, 1942

Model	Angle of afterbody keel, α, deg.
126B-1	4
126B-2	6-1/4
126B-3	8-1/2

Angle of dead rise, 19°. Date of test Feb., 1942

Model	Angle of afterbody keel, α, deg.
126C-1	4
126C-2	6-1/4
126C-3	8-1/2

Angle of dead rise, 23-1/4°. Date of test July, 1942

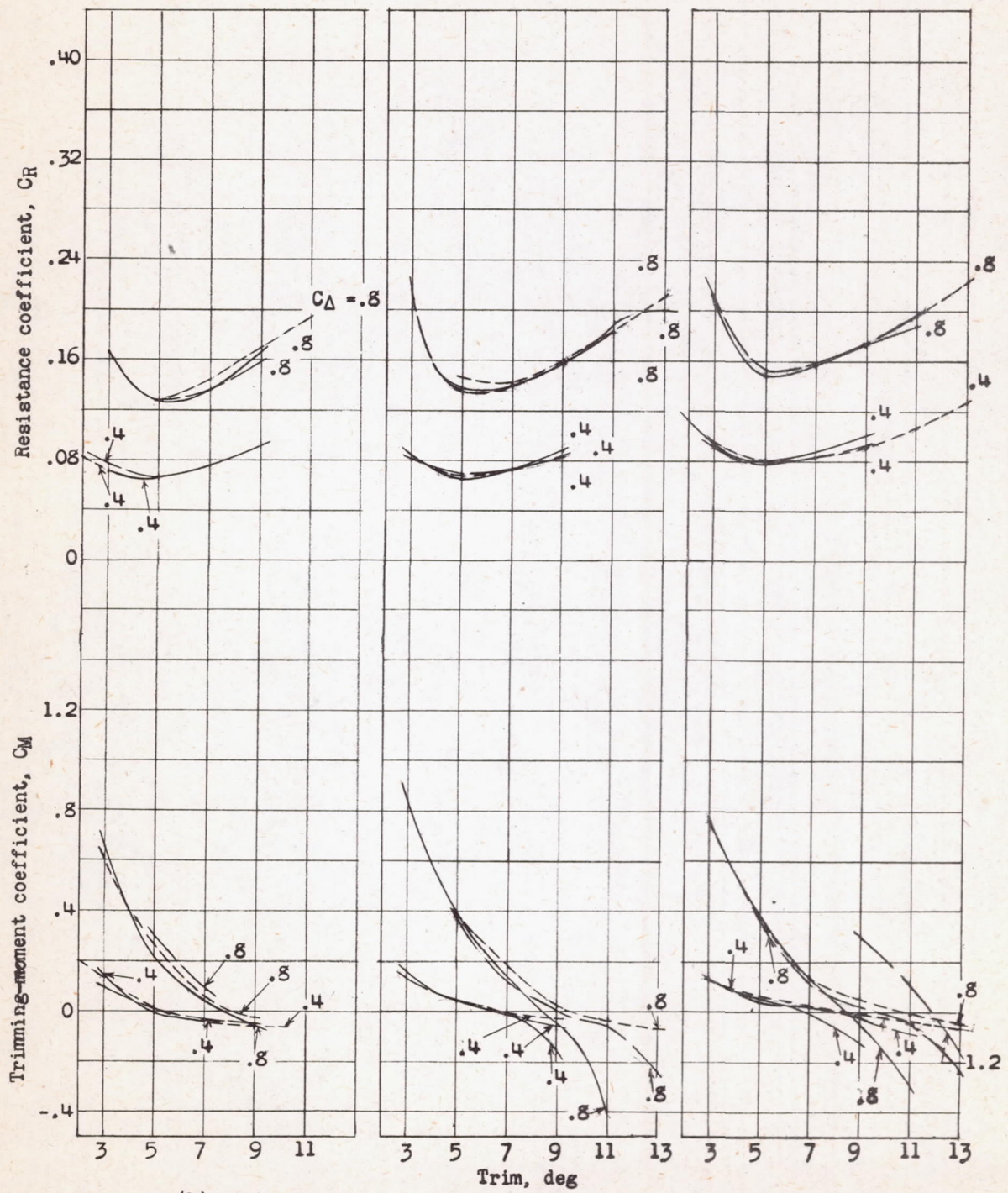

(b) At C_V = 4.5.

Figure 7. - Continued.

Model	Angle of afterbody keel, α, deg.	Model	Angle of afterbody keel, α, deg.	Model	Angle of afterbody keel, α, deg.
126A-1	4	126B-1	4	126C-1	4
126A-2	6-1/4	126B-2	6-1/4	126C-2	6-1/4
126A-3	8-1/2	126B-3	8-1/2	126C-3	8-1/2

Angle of dead rise, 14-3/4°. Date of test July, 1942

Angle of dead rise, 19°. Date of test Feb., 1942

Angle of dead rise, 23-1/4°. Date of test July, 1942

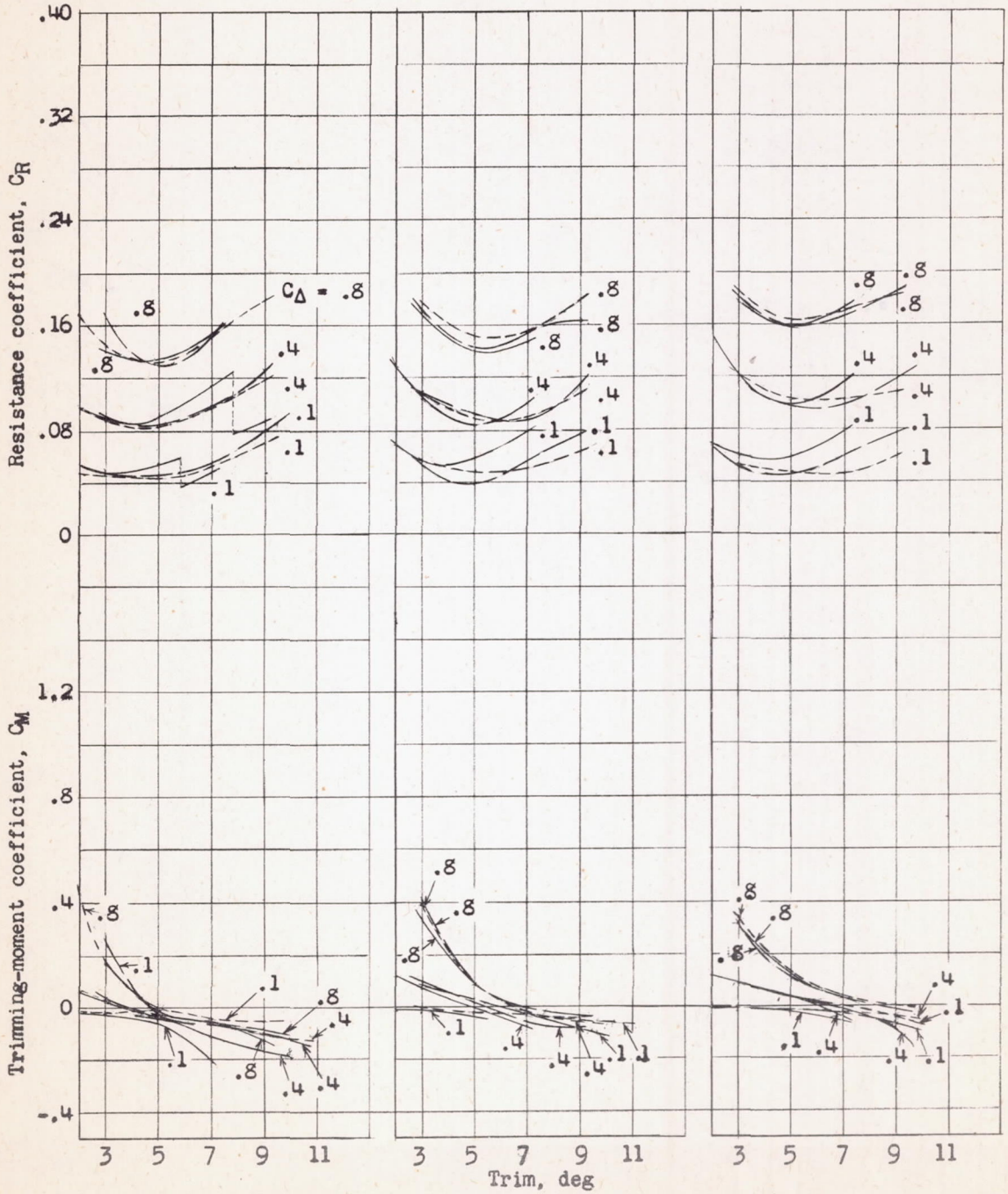

(b) At C_Y = 6.0.

Figure 7. - Continued.

I-305

Model	Angle of afterbody keel, α, deg.
126A-1	4
126A-2	6-1/4
126A-3	8-1/2

Model	Angle of afterbody keel, α, deg.
126B-1	4
126B-2	6-1/4
126B-3	8-1/2

Model	Angle of afterbody keel, α, deg.
126C-1	4
126C-2	6-1/4
126C-3	8-1/2

Angle of dead rise, 14-3/4°. Date of test July, 1942

Angle of dead rise, 19°. Date of test Feb., 1942

Angle of dead rise, 23-1/4°. Date of test July, 1942

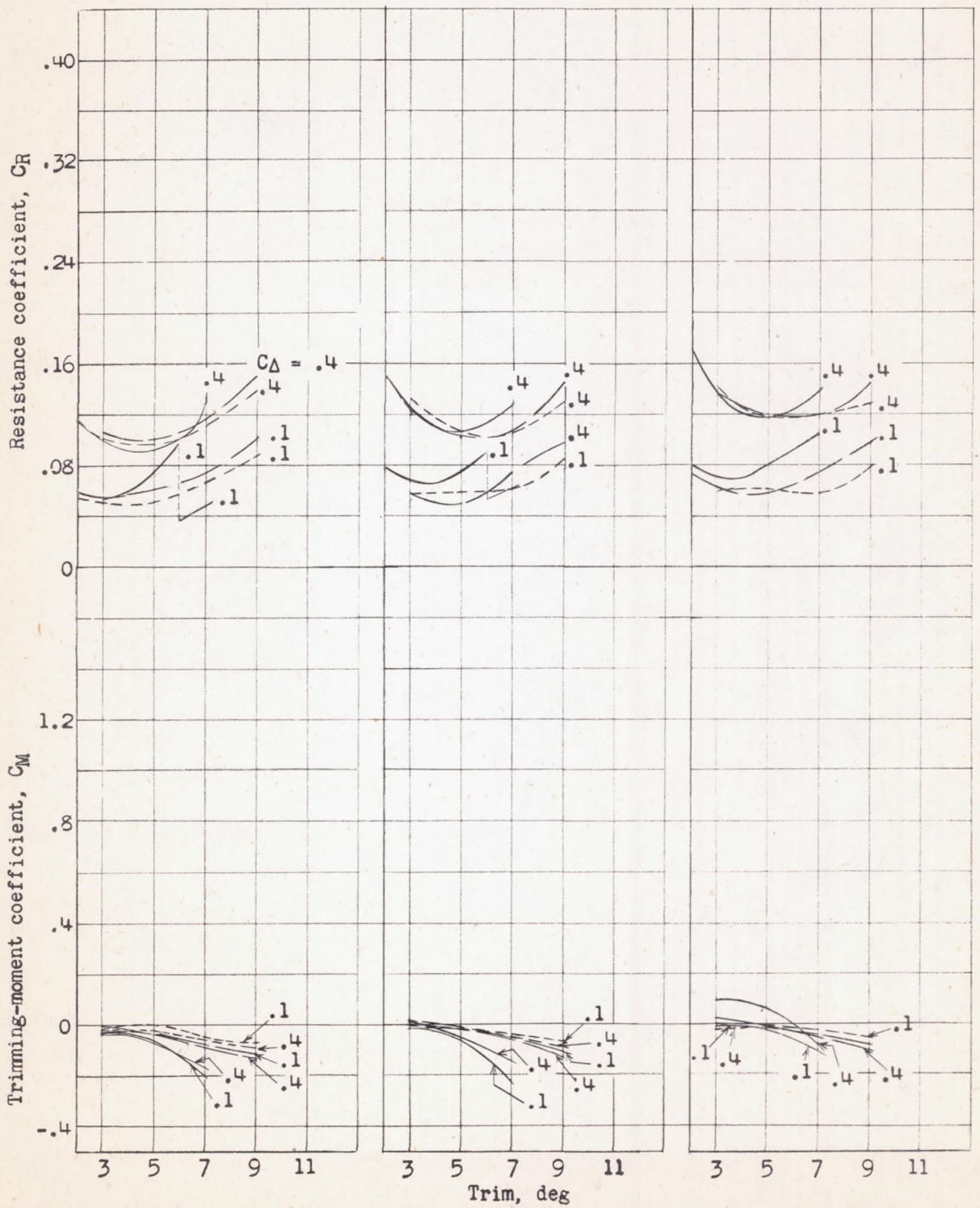

(d) At Cv = 7.0.

Figure 7. - Concluded.

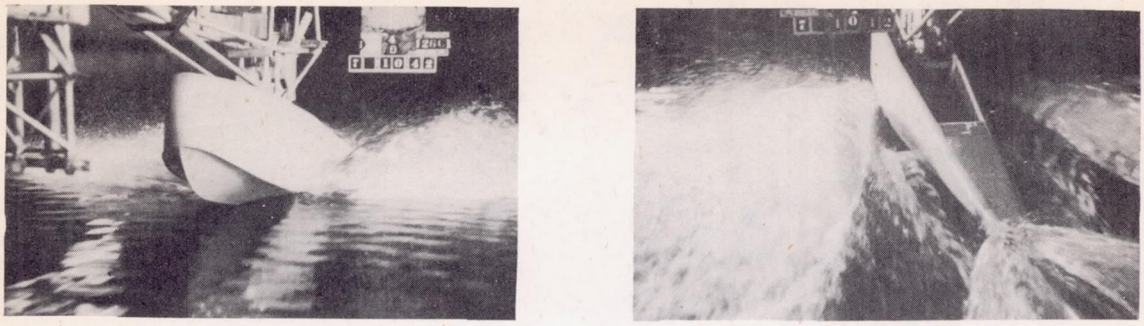

Model 126C-1. Angle of afterbody keel, 4°.

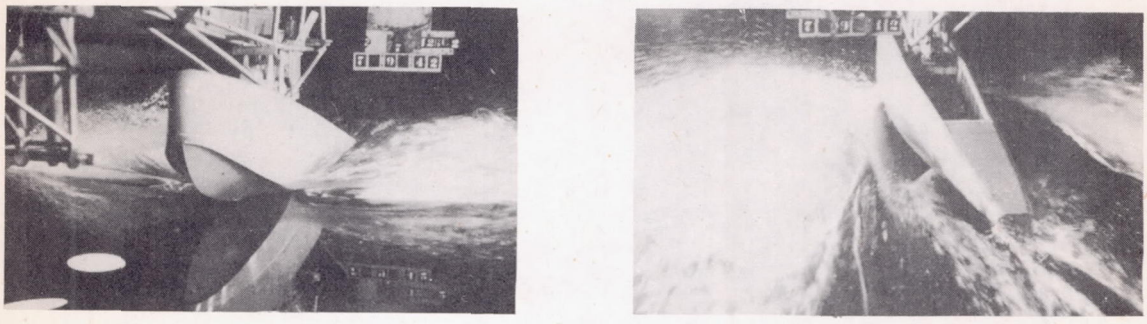

Model 126C-2. Angle of afterbody keel, 6° 15'.

Model 126C-3. Angle of afterbody keel, 8° 30'.

Figure 8.- Effect of angle of afterbody keel on spray at hump speed. C_V = 3.0 (approximately); 11° fixed trim; C_Δ = 1.027; angle of dead rise, 23° 16'.

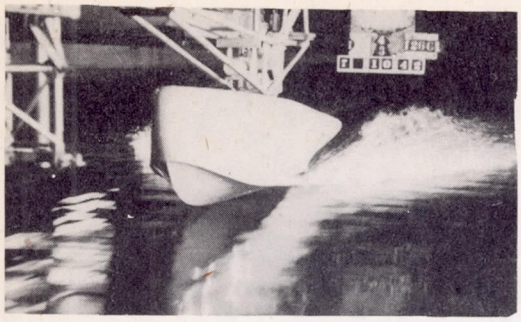

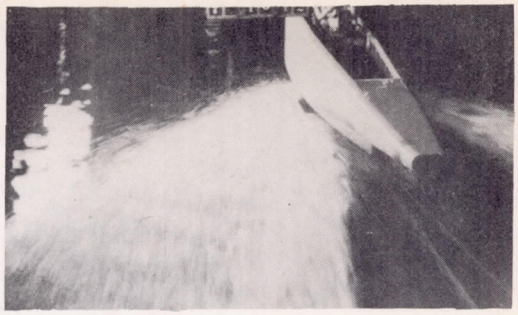

Model 126C-1. Angle of afterbody keel. 4°.

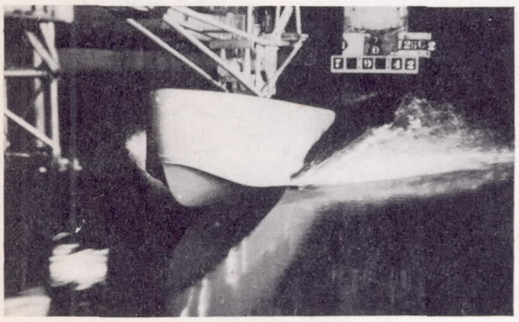

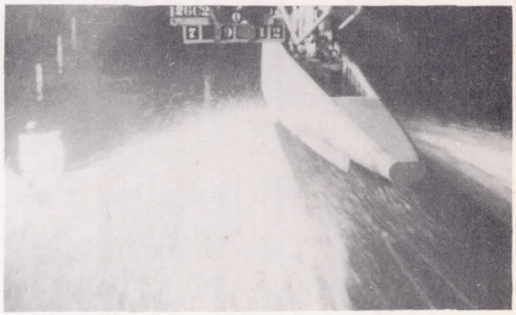

Model 126C-2. Angle of afterbody keel, 6° 15'.

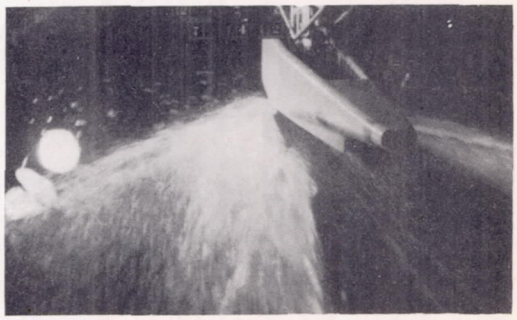

Model 126C-3. Angle of afterbody keel, 8° 30'.

Figure 9. - Effect of angle of afterbody keel on spray at planing speed C_V = 5.0 (approximately); 5° fixed trim; C_Δ = 1.027; angle of dead rise, 23° 16'.

L-305

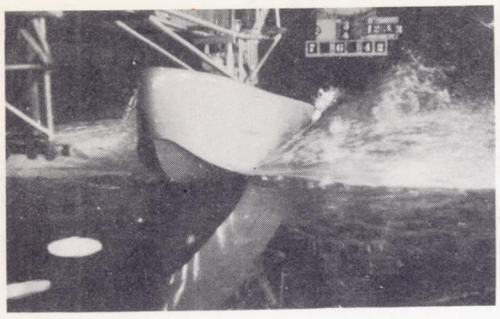

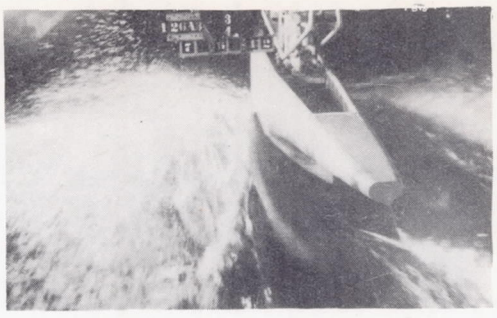

Model 126A-3. Angle of dead rise, 14° 44'.

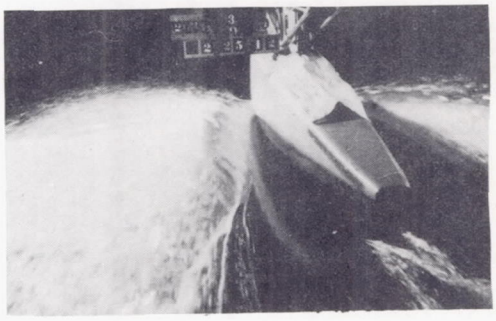

Model 126B-3. Angle of dead rise, 19°.

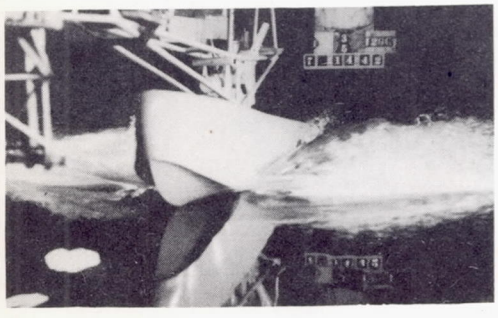

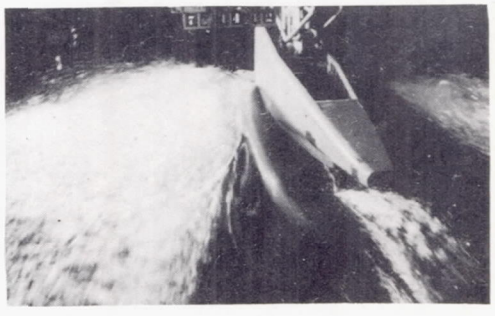

Model 126C-3. Angle of dead rise, 23° 16'.

Figure 10.- Effect of angle of dead rise on spray at hump speed. C_V = 3.0 (approximately); 9° fixed trim; C_Δ = 1.027; angle of afterbody keel, 8° 30'.

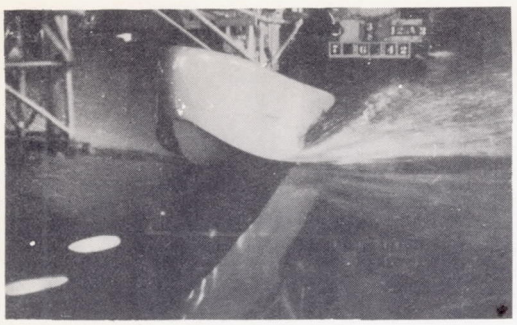

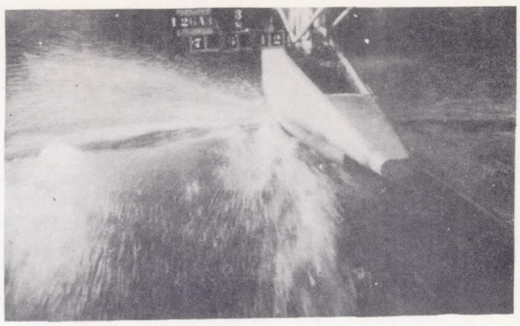

Model 126A-3. Angle of dead rise, 14° 44'.

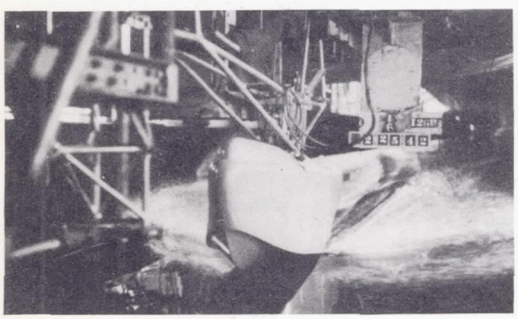

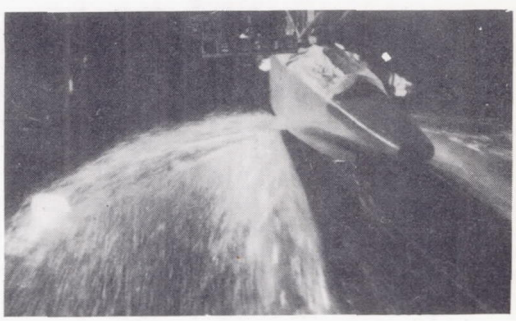

Model 126B-3. Angle of dead rise, 19°.

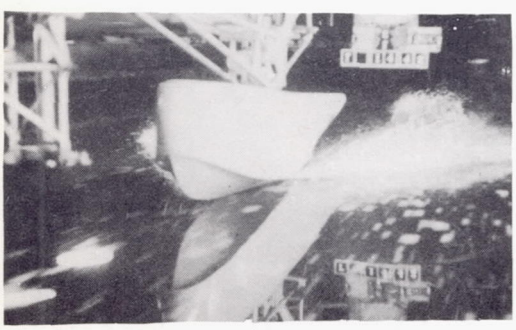

Model 126C-3. Angle of dead rise, 23° 16'.

Figure 11.- Effect of angle of dead rise on spray at planing speed. C_V = 5.0 (approximately); 5° fixed trim; C_Δ = 1.027; angle of afterbody keel, 8° 30'.

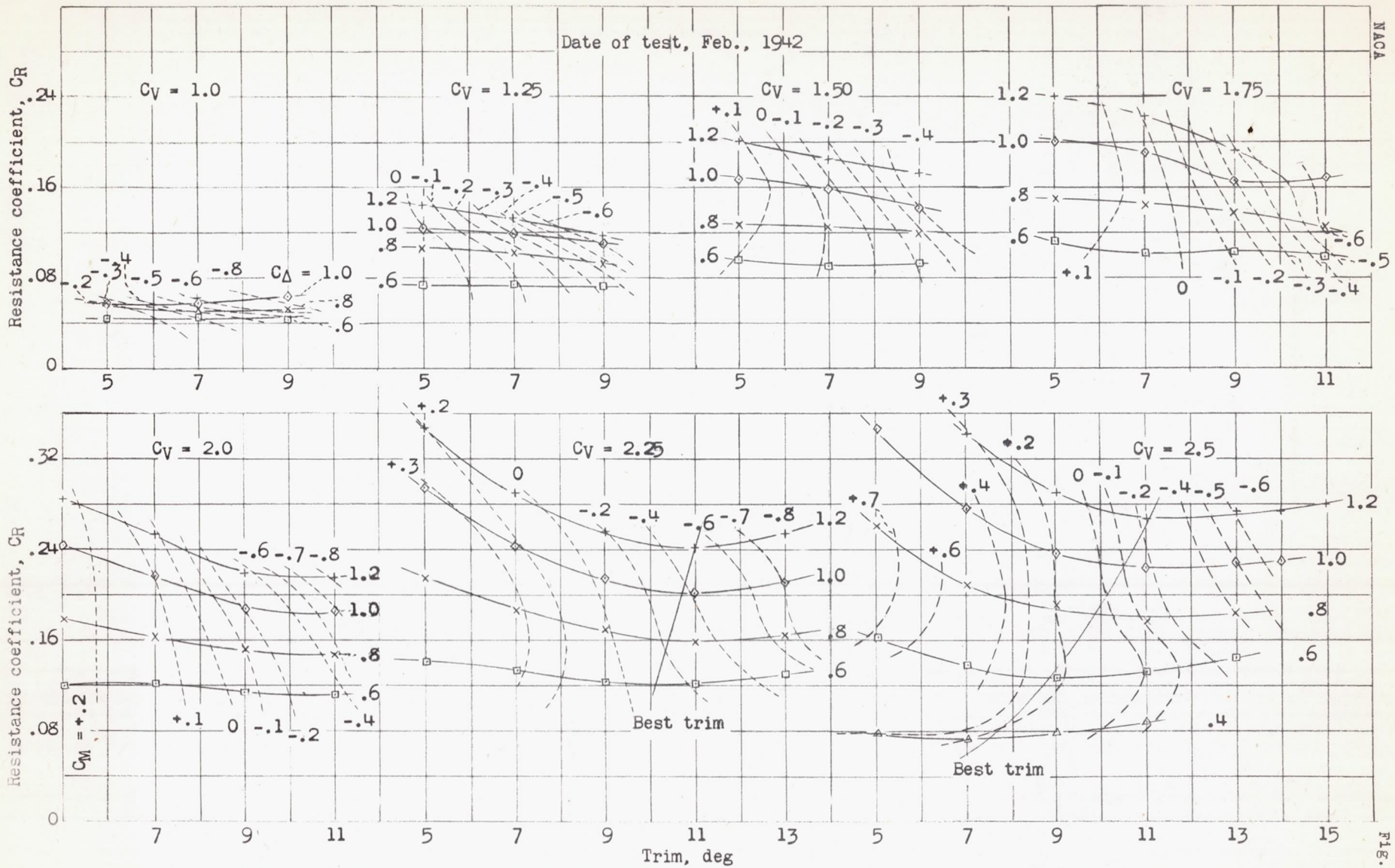

Figure 12.- Model 126B-2. Working charts for the determination of resistance and trimming moment. Angle of dead rise, 19°.
(a) Angle of afterbody keel, 6-1/4°. (1 block = 10/32")

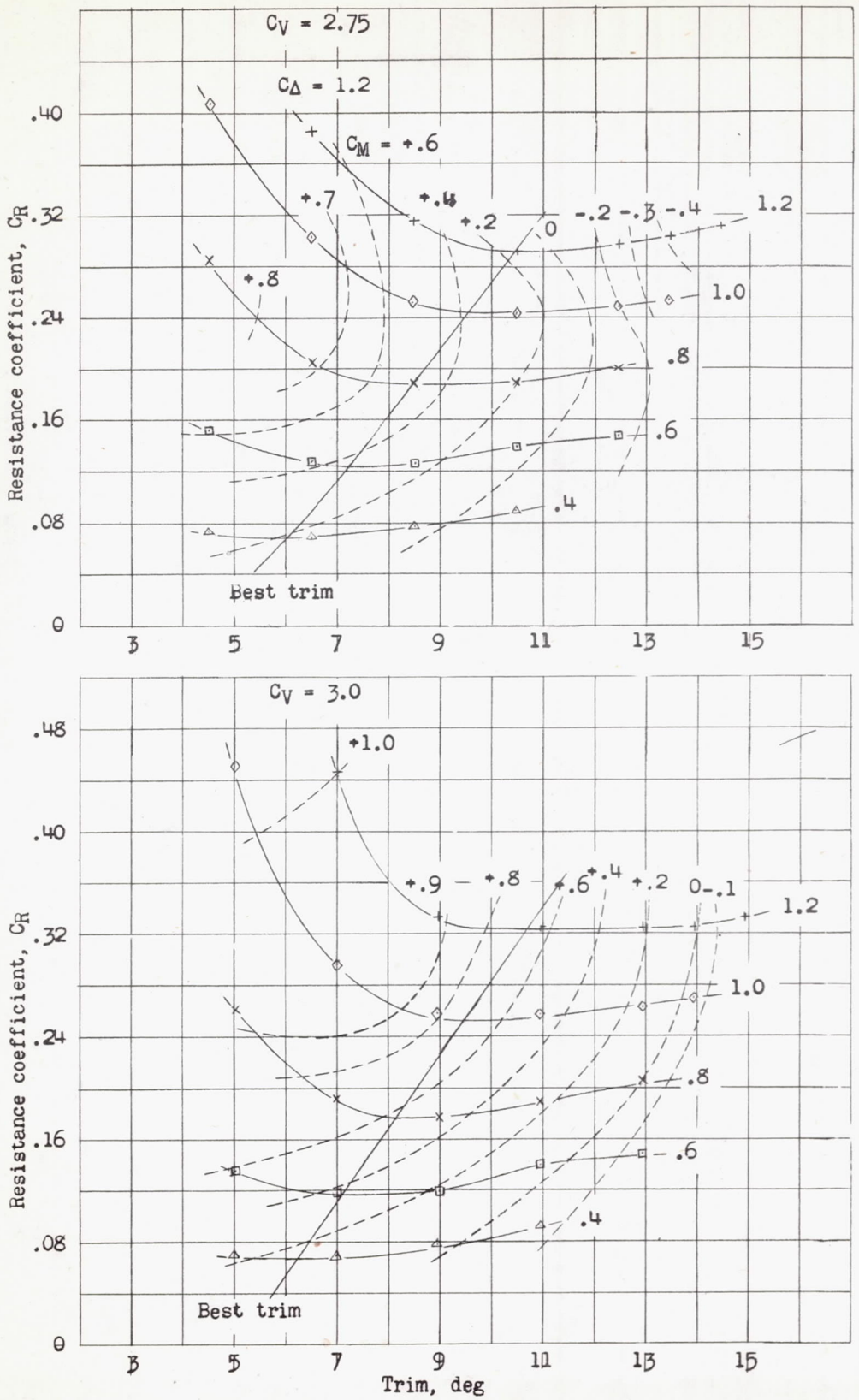

(1 block = 10/32")

Figure 12.- Continued.
(b)

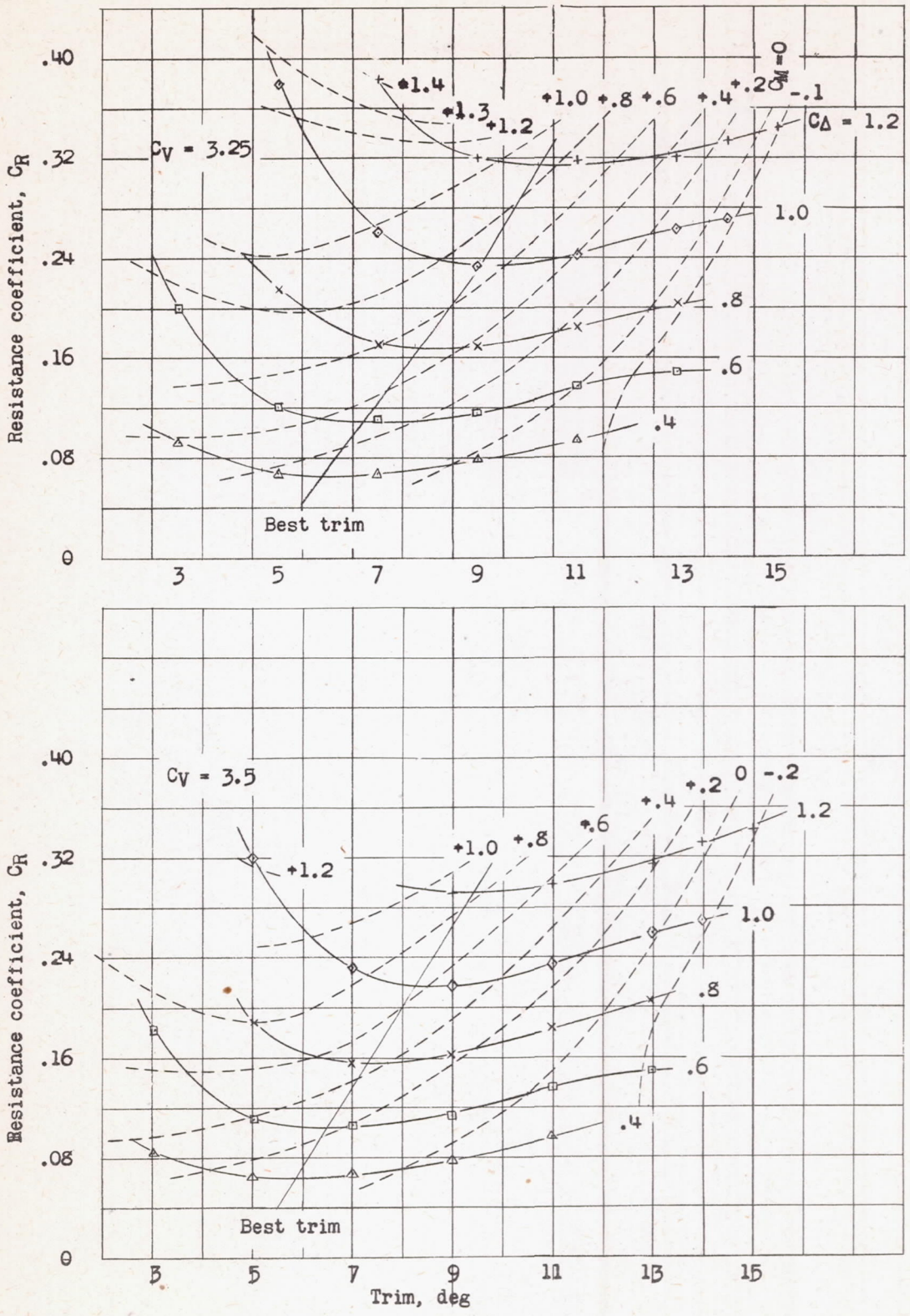

Figure 12.- Continued.
(c)

L-305

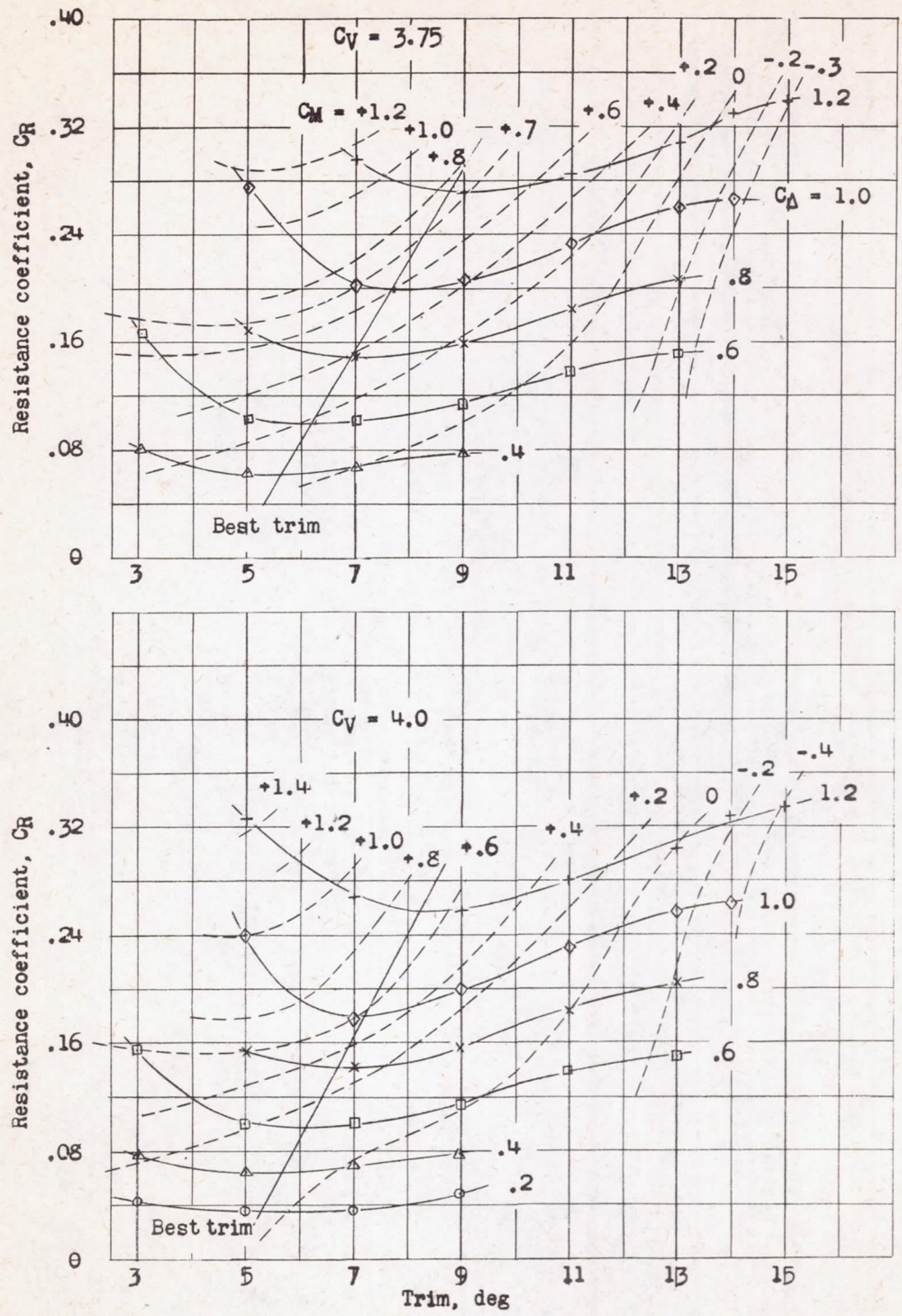

(1 block = 10/32")

Figure 12.- Continued.
(d)

L-305

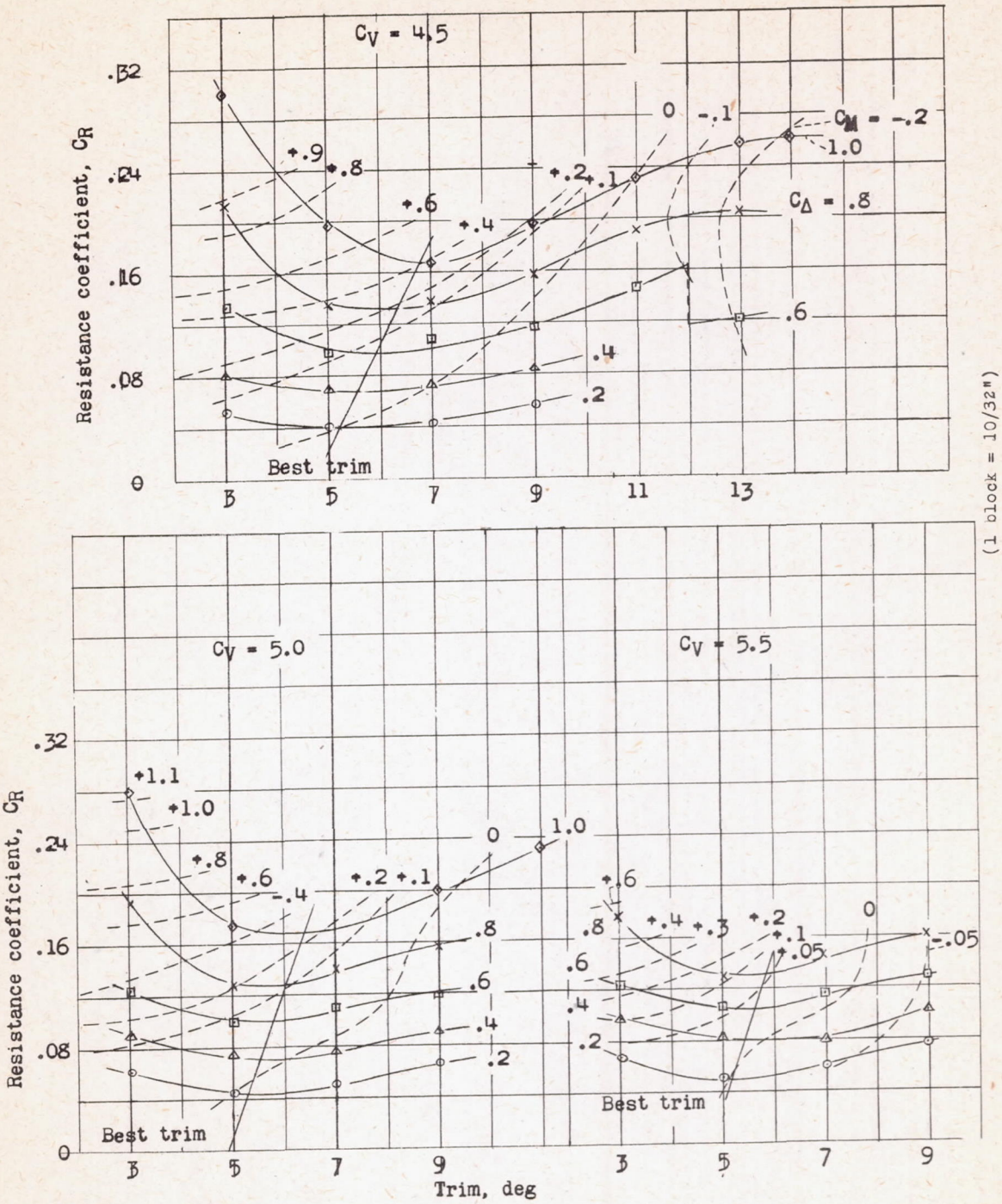

Figure 12.- Continued.
(e)

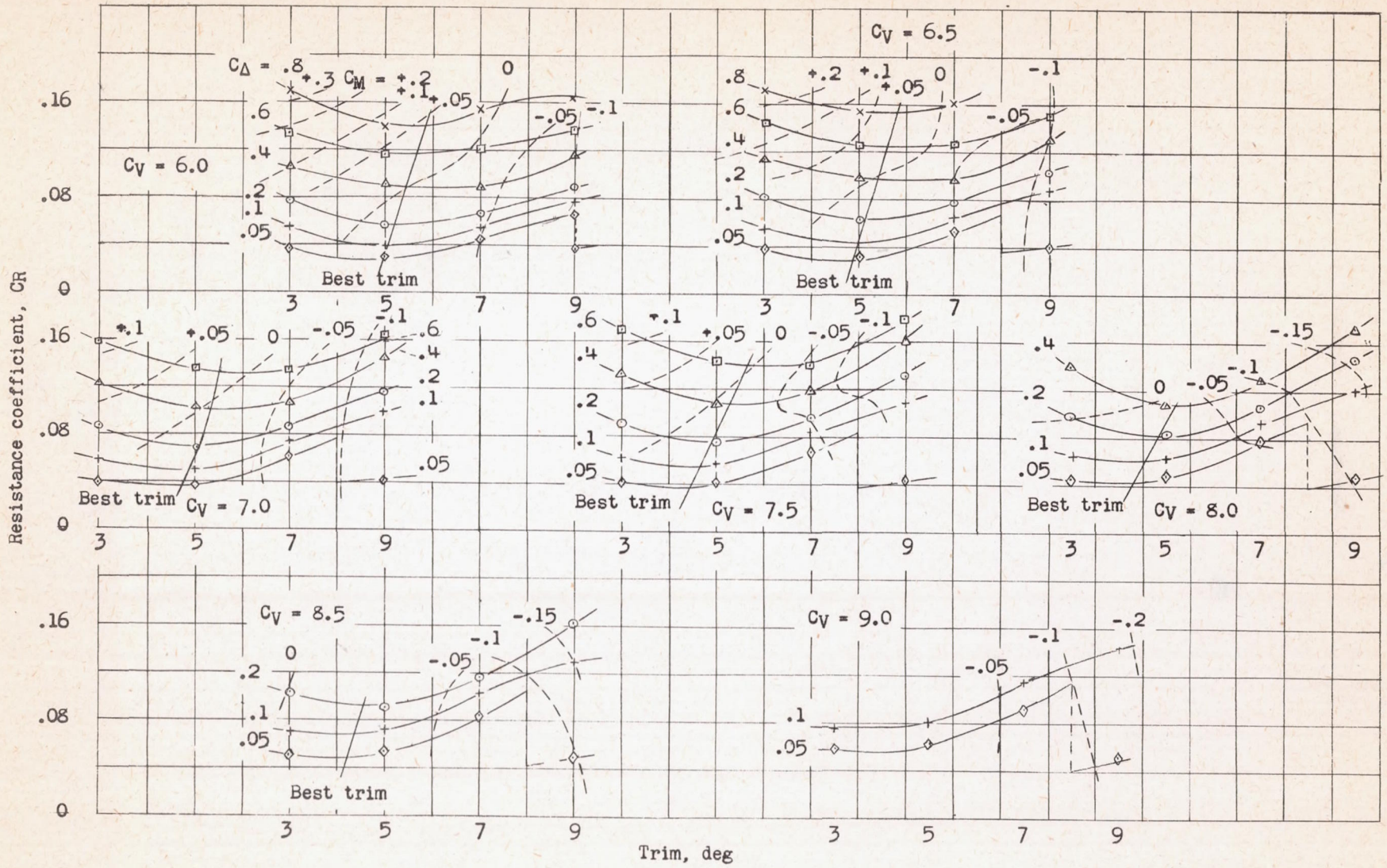

Figure 12.- Concluded.
(f)

(1 block = 10/32 on Arch. scale)

NACA

Fig. 12f

L-305

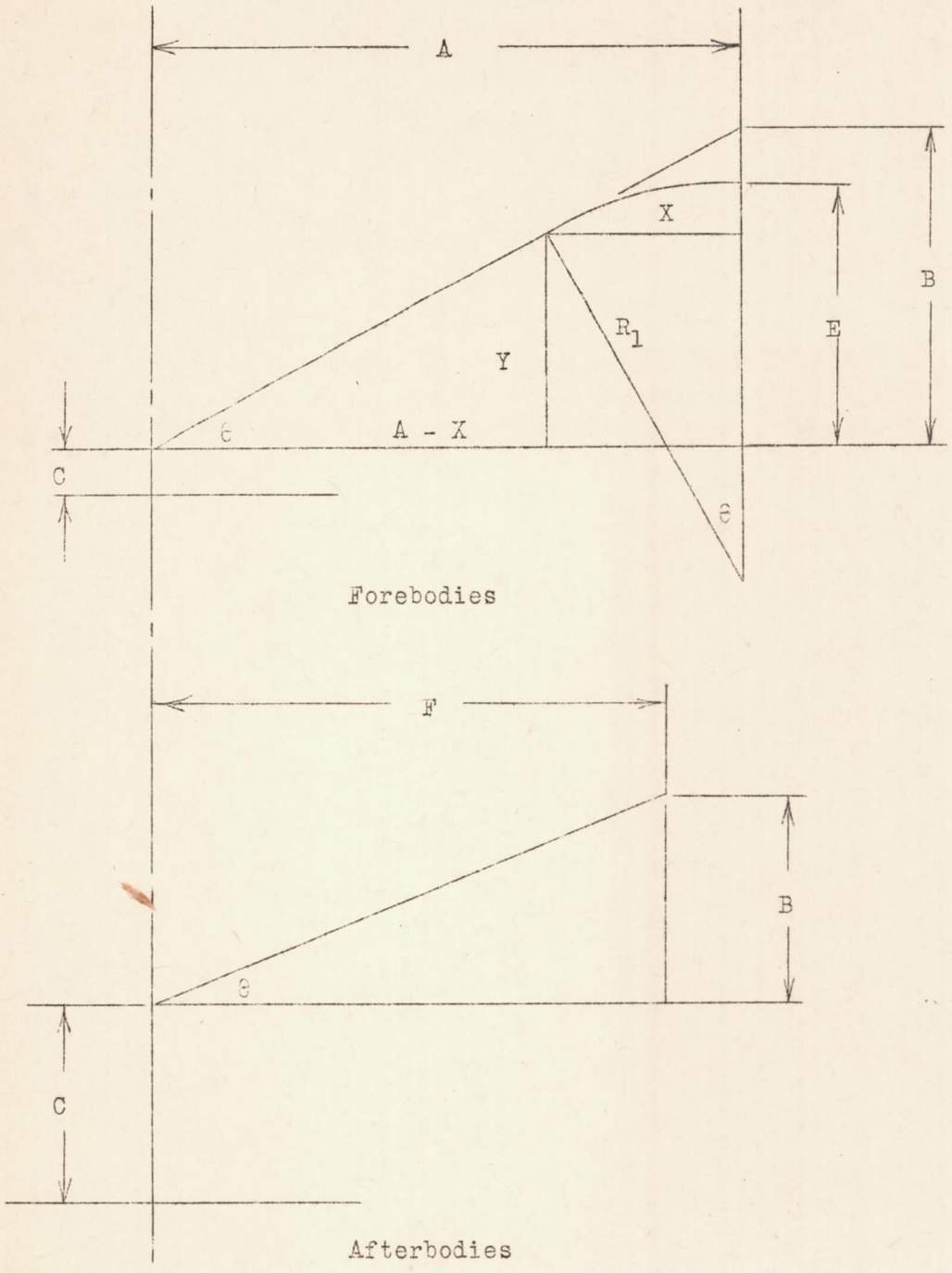

Figure 13.- Diagram illustrating the method used for the derivation of stations of Models 126A and 126C.